

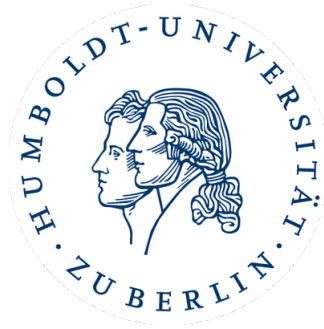
Hedging strategies under jump-induced market incompleteness

Master's Thesis submitted to

Prof. Dr. Wolfgang Härdle
Prof. Dr. Natalie Packham

School of Business and Economics
Ladislaus von Bortkiewicz Chair of Statistics

Humboldt Universität zu Berlin



by

Jovanka Matic

554474

in partial fulfillment of the requirements for the degree of
Master of Science in Statistics

Berlin, September 1, 2019

Acknowledgement

I would like to express my sincere gratitude to my supervisor Prof. Dr. Wolfgang K. Härdle for his support, inspiration, mental support and belief during this thesis.

I would like to express my sincere gratitude to my second supervisor Prof. Dr. Natalie Packham for her guidance, patience and time invested in this project.

I like to thank my family and friends for supporting me during this thesis. I am most grateful to my mother.

Abstract

The market for cryptocurrencies is a very dynamic market with highly volatile movements and discontinuities from large jumps. We investigate the risk-management perspective when selling securities written on cryptocurrencies. To this day, options written on cryptocurrencies are not officially exchange-traded. This study mimics the dynamics of cryptocurrency markets in a simulation study. We assume that the asset follows the stochastic volatility with correlated jumps model as presented in Duffie et al. (2000) and price options with parameters calibrated on the CRIX, a cryptocurrency index that serves as a representative of market movements. We investigate on risk-management opportunities of hedging options written on cryptocurrencies and evaluate the hedge performance under model misspecification. The hedge models are misspecified in the manner that they include fewer sources of randomness than the data-generating process. We hedge with the industry-standard Black-Scholes option pricing model, the Heston Stochastic volatility model, and the Merton jump-diffusion model. We present different hedging strategies and perform an empirical study on delta-hedging. We report poor hedging results when calibration is poor. The results show good performances of the Black-Scholes and the Heston model and outline the poor hedging performance of the Merton model. Lastly, we observe large unhedgeable losses in the left tail. These losses potentially result from large jumps.

Contents

List of Figures	v
List of Tables	vi
1 Introduction	1
1.1 Literature review	3
2 Pricing	4
2.1 Market setup	4
2.2 Arbitrage theory	4
2.3 Simplifications compared to real-world case	6
2.4 Pricing model	6
2.4.1 Market incompleteness	7
2.4.2 Option pricing	8
2.5 Discretization	9
2.5.1 Calibration	10
3 Hedging	12
3.1 Hedging in discrete time	13
3.2 Hedge models	13
3.2.1 Black-Scholes asset pricing model	13
3.2.2 Heston stochastic volatility model	16
3.2.3 Merton Jump diffusion model	18
3.3 Quadratic hedging	19
3.4 Hedge model calibration	20
4 Simulation study	23
4.1 Calibration of hedge models	23
5 Hedge performance of dynamic delta hedging	27
5.1 Black-Scholes	27
5.2 Heston model	31
5.3 Merton jump diffusion	34
5.4 Comparison of Δ -hedges	36
6 Conclusion	37
A Appendix	38
A.1 Derivation of the Fourier transform of the damped call price	38
A.2 Tables	39

List of Figures

1	CRIX historical time series	1
2	25 Euler discretized trajectories of $S(t)$ for a time horizon of 1 year	11
3	4000 simulated trajectories of $S(t)$ with jumps in returns and volatility in 3a and without jumps in 3b	12
4	SVCJ implied volatility surface for 77 options	24
5	Implied volatility surface of the Heston model	25
6	Implied volatility surface of the Merton model	26
7	Trajectories of the misspecified delta Δ_{BS} in blue compared to the trajectory of the underlying $S(t)$ in red	27
8	Relative PnL for 9M under misspecification with Black-Scholes for K_{ATM}	30
9	Trajectories of the misspecified delta Δ_{SV} in blue compared to the trajectory of the underlying $S(t)$ in red	31
10	Relative PnL for 9M under misspecification with Heston for K_{ATM}	33
11	Trajectories of the misspecified delta Δ_{Merton} in blue compared to the trajectory of the underlying $S(t)$ in red	34
12	Relative PnL for $\tau = 9M$ under misspecification with Merton for K_{ATM}	36

List of Tables

1	SVCJ calibrated parameters of the CRIX from Hou et al. (2019). Red means strong positive significance (below 0.001 %) and blue strong means negative significance (below 0.001 %)	10
2	Simulated ATM option prices for 11 maturities	23
3	Calibrated parameter of the Black-Scholes model	24
4	Calibrated parameters of the Heston model	25
5	Calibrated parameters of the Merton model	26
6	Quantiles of the Profit and Loss distribution where the hedge model is Black-Scholes for K_{ATM}	29
7	Selected moments and the hedge error where the Hedge model is Black-Scholes for K_{ATM}	30
8	Quantiles of the Profit and Loss distribution where the Hedge model is Heston ATM .	32
9	Selected moments and the hedge error where the Hedge model is Heston for K_{ATM} .	32
10	Quantiles of the Profit and Loss distribution where the Hedge model is Merton ATM .	35
11	Selected moments and the hedge error where the Hedge model is Merton for K_{ATM} .	35
12	Option pricing with Monte Carlo option pricing for 7 strikes and 11 maturities	39
13	Option pricing with Monte Carlo option pricing for 7 strikes and 11 maturities	40
14	Quantiles of the relative P &L distribution where the Hedge model is Black-Scholes for $K_{0.95}$	41
15	Selected moments and the hedge error where the Hedge model is Black-Scholes for $K_{0.95}$	41
16	Quantiles of the relative P &L distribution where the Hedge model is Black-Scholes for $K_{1.05}$	42
17	Selected moments and the hedge error where the Hedge model is Black-Scholes for $K_{1.05}$	42
18	Quantiles of the relative Profit and Loss distribution where the Hedge model is Merton for $K_{0.95}$	43
19	Selected moments and the hedge error where the Hedge model is Merton for $K_{0.95}$. .	43
20	Quantiles of the relative Profit and Loss distribution where the Hedge model is Merton for $K_{1.05}$	44
21	Selected moments and the hedge error where the Hedge model is Merton for $K_{1.05}$. .	44
22	Quantiles of the relative Profit and Loss distribution where the Hedge model is Heston for $K_{0.95}$	45
23	Quantiles of the relative Profit and Loss distribution where the Hedge model is Heston for $K_{1.05}$	45

1 Introduction

In 2017, an emerging market caught the eye of the general public and the financial world. The rise of cryptocurrencies attracted high media attention. Everyday citizen as well as financial institutions entered the market with the prospect of benefiting from the large upward movements in prices. The boom ended in the first quarter of 2018 and the media presence has vanished. Bitcoin, by far the most famous and largest cryptocurrency was initially introduced in the White Paper by the pseudonym Nakamoto (2008) and is circulated since 2009. A cryptocurrency is a decentralized digital circulating medium with the property that transactions are regulated through cryptography (Härdle and Trimborn, 2019). This paper considers the financial aspects of trading assets like cryptocurrencies and does not focus on their macroeconomic or technological aspects. For further details on the listed topics, the reader is referred to an overview in Härdle and Reule (2019).

The purpose of this paper is to analyze financial risk in a market that aims to mimic the movements of cryptocurrencies such as Bitcoin, Ethereum, Ripple and some other cryptocurrencies. This paper considers the information about the movement on cryptocurrency markets based on a representative benchmark. Trimborn and Härdle (2018) define and introduce the CRyptocurrency IndeX (CRIX). The CRIX is a weighted cryptocurrency index with a floating number of constituents that are redefined in cycles of 3 months. The market capitalization of each cryptocurrency involved determines the weight. The CRIX is reallocated monthly. For more information on the methodology, the reader is referred to Trimborn and Härdle (2018) and is invited to visit the website www.thecrix.de. A few studies have investigated the movements of the CRIX. As an example, Chen et al. (2018) investigate the dynamics of the CRIX with traditional econometric methods such as time series analysis.

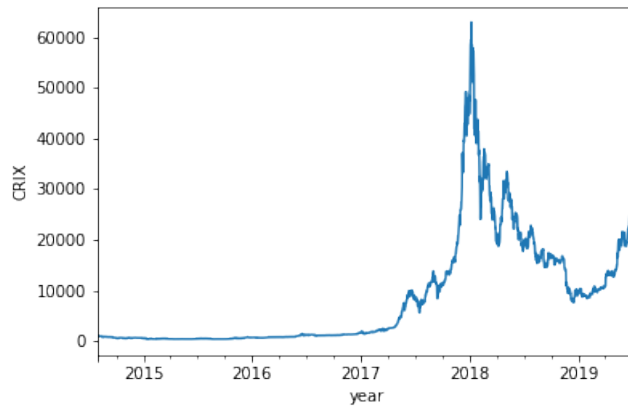


Figure 1: CRIX historical time series

 CrixToDate

At this point, cryptocurrency contingent claims are not officially exchange-traded. Hou et al. (2019) contribute to the pricing of European-style options. They attempt to price cryptocurrency options

written on CRIX and Bitcoin with the Stochastic Volatility with correlated jumps (SVCJ) option pricing model introduced in Duffie et al. (2000) and the co-jump model by Bandi and Reno (2016). This paper is an extension to the work of Hou et al. (2019). It investigates hedging strategies for plain vanilla European-style option prices that are priced under the SVCJ. The pricing and hedging are based on an option writer’s perspective. For example, it could be some bank or any financial institution willing to offer cryptocurrency options. Green and Figlewski (1999) address the asymmetric risk exposure between option writers and buyers. From a buyer’s perspective, the loss is limited to the premium paid for the option. On the contrary, the seller is exposed to various risk factors including losses that can vastly exceed the initial premium collected (Green et al., 1999). This is just one illustration among many that outlines why financial market risk management is equally as important as pricing. Furthermore, risk management, in our case hedging, contributes to a deeper understanding of price and market dynamics. It helps to identify risk factors and their contribution to the P&L (Bergomi, 2015). The following quote from Bergomi (2015) puts this accurately on point:

”...again, the issue, from a practitioners perspective, is not to be able to predict anything, but rather to be able to differentiate risks generated by these different contributions to his/her P&L and to ensure that the model offers the capability of pricing these different types of risk consistently across the book at levels that can be individually controlled. It is then a trading decision to either hedge away some of these risks, by taking offsetting positions in more liquid say vanilla options or by taking offsetting positions in other exotic derivatives, or to keep these risks on the book.”

Quote on hedging in (Bergomi, 2015, p.2).

The hedging procedure in this paper is related to the work of Branger et al. (2012) and Sun et al. (2015). This paper assumes that the dynamics of the asset price process follow the SVCJ model under the parameters calibrated by Hou et al. (2019). We hedge under model misspecification. In the context of our study, a hedge model is defined as the model that determines the portfolio strategy of the hedge portfolio. The hedge models under consideration are misspecified in the manner that they include fewer sources of randomness than the data-generating process SVCJ.

Branger et al. (2012) name this procedure the omittance of risk factors. The hedge models under consideration are the same as selected by Branger et al. (2012) and Sun et al. (2015). Precisely, the hedge models in this study are: the Merton (1976) Jump-diffusion model (Merton model), the Heston (1993) Stochastic Volatility model (Heston model) and the Black-Scholes (‘classic’ Black-Scholes) asset pricing model introduced by Black and Scholes (1973). Throughout this paper, the Black-Scholes model will be referred to as the ‘classic’ Black-Scholes (El Karoui et al., 1998). The properties of these hedge models under consideration are reviewed in section 3. We believe that the selected hedging procedure relates to what a trader or practitioner would do. A trader would observe the unspecified dynamics of the underlying asset and initially proceed with the simplest model at hand. This is generally the industry-standard ‘classic’ Black-Scholes asset pricing

model (Green et al., 1999). He would then extend the model assumptions to modifications of Black-Scholes and include additional sources of randomness such as jumps and/or stochastic volatility to both his pricing or hedging strategy (Green et al., 1999). We try to evaluate the performance of this hedging strategy for a market that imitates the behavior of cryptocurrency assets.

This paper is structured as follows: section 1.1 reviews existent literature, section 2 defines the market setup and reviews the pricing model, section 3 reviews the hedging models and defines the hedging strategies, section 4 presents the results from the delta-hedging simulation study, section 5 evaluates the performance from hedging and section 6 concludes.

1.1 Literature review

Several studies investigate the hedge performance of misspecified hedge models. Branger et al. (2012) investigate the hedge performance under model simplification. The asset price follows the Stochastic Volatility with jumps (SVJ) model by Bakshi et al. (1997). They perform a delta, delta-vega and minimum variance hedge with the 'classic' Black and Scholes (1973), the Merton (1976) model and the Heston (1993) model and compare the performance of the hedge with the actual model. Their findings suggest that in terms of delta-hedging, the classic Black-Scholes outperforms other models. However, the model performs poorly during extreme periods (Branger et al., 2012). In this paper, the listed observation is evaluated in detail in section 3. Branger et al. (2012) report that the Heston model is the best performing model among all models. In a nutshell, Branger et al. (2012) interpret the hedge results as follows: The hedge performance of the Heston model is sophisticated during regular periods ("normal times"), but poor during large market movements ("extreme events"). On the contrary, the Merton (1976) model provides a sophisticated hedge during "extreme events", but behaves poorly in regular periods. The data-generating process in this framework distinguishes itself from the SVJ because it incorporates jumps in volatility that are correlated to jumps in returns. This is an additional source of randomness. The dynamics of the underlying are described in detail in section 2.4. Sun et al. (2015) apply the same misspecification in terms of fewer sources of randomness in the hedge models. In their simulation study, the data-generating process follows the double Heston jump-diffusion model. They investigate between "having a lucky guess of the market model, or having a good fit hedging model" (Sun et al., 2015). In terms of hedging accuracy, the study shows that a misspecification of the hedge model has an insignificant impact on the hedging performance, whereas the accurate calibration of hedge models drastically increases the hedge performance under model misspecification. This is in line with the findings of Green et. al (1999). They investigate the risk exposure from model risk in cases of mispricing and incorrect volatility estimation or forecasting. Under the assumption that an option is priced according to the industry standard 'classic' Black-Scholes, Green et al. (1999) find that the risk exposure resulting from model risk is material or severe. They recommend a "volatility markup" for pricing put options. However, this markup is not recommended for hedging (Green et. al., 1999). El Karoui et al. (1998) investigate hedging under misspecification in volatility. They investigate the hedging stochastic volatility models with the

'classic' Black-Scholes option pricing model. They show that under certain circumstances, the popular Black-Scholes option pricing model provides a robust hedge. The hedge performance is robust under convexity of the claim and an accurate volatility fit.

2 Pricing

2.1 Market setup

This paper considers a frictionless and continuous-time financial market denoted by $\mathcal{M} = \{(\Omega, \mathcal{F}, \mathcal{F}_t, P), T, (S, B)\}$. The mathematical notation is related to Franke et al. (2015), El Karoui et al. (1998), Hilpisch (2015) and Detering and Packham (2015). The time horizon $T \in [0, \infty)$ is fixed and the interest rate $r \geq 0$ is assumed to be constant. On a filtered probability space $(\Omega, \mathcal{F}, (\mathcal{F}_t)_{t \in [0, T]}, P)$ are defined a strictly positive deterministic risk-free asset $(B(t))_{t \geq 0}$ with $B(0) = 1$ and $B(t) = e^{rt}$, $t \in [0, T]$ and a semi-martingale $\tilde{S} = \tilde{S}(t)_{0 \leq t \leq T}$ adapted to a filtration $\{\mathcal{F}_t, t \geq 0\}$ satisfying the 'usual conditions'. We express the asset prices in units of $\tilde{S}_0(t) = \tilde{S}(0)B(t)$. The value of the asset at time t is $S(t) = \left(\frac{\tilde{S}(t)}{\tilde{S}_0(t)} \cdot 100\right)$, $0 \leq t \leq T$, where $S(0) = 100$. The dynamic portfolio strategy $\phi = (\phi_0, \phi_1) = (\phi_0(t), \phi_1(t))_{0 \leq t \leq T}$ is an \mathcal{F} -predictable process. $\phi_0(t)$ represents the number of assets held in the risk-free asset and $\phi_1(t)$ denotes the number of assets held in $S(t)$. The value of the portfolio at time t is

$$V_\phi(t) = \phi_0(t)B(t) + \phi_1(t)S(t) \quad (1)$$

$V_\phi(0)$ denotes the initial value of the portfolio. In this financial market, we allow borrowing and short-selling. However, we impose the requirement that the investor must be able to repay debt at any time (Jeanblanc et al., 2009). We require our portfolio to be admissible. Formally, there exists constant α such that $V_\phi(t) \geq -\alpha$ almost surely for every $t \leq T$. A portfolio is self-financing if

$$dV_\phi(t) = \phi_0(t)dB(t) + \phi_1(t)dS(t) \quad (2)$$

The interpretation of equation (2) is that gains result from changes in the underlying $S(t)$ and not from realignments of the portfolio (Jeanblanc et al., 2009). At time t , the self-financed value of the portfolio $V_\phi(t)$ solves

$$dV_\phi(t) = r[V_\phi(t) - \phi_1(t)S(t)]dt + \phi_1(t)dS(t) \quad (3)$$

2.2 Arbitrage theory

This financial market is assumed to be free of arbitrage. We briefly summarize selected fundamental concepts of arbitrage theory and risk-neutral pricing. The theoretical review is based on Shreve (2004), Franke et al. (2015), Jeanblanc (2009), Hilpisch (2014) and Cont and Tankov (2003). We open the stage with the definition of a risk-neutral measure P_Q . Let P denote the historical probability measure.

A probability measure P_Q is risk-neutral if

1. P_Q is equivalent to P . Formally, $\forall A \in \mathcal{F}, P(A) = 0 \iff P_Q(A) = 0$
2. the discounted asset price $S(t)$ is a martingale under P_Q

Theorem 1 (Martingale representation theorem). *Let $\{W(t), 0 \leq t \leq T\}$ be a Wiener process on (Ω, \mathcal{F}, P) and let \mathcal{F} be the filtration generated by this Wiener process. $M(t), 0 \leq t \leq T$ denotes a martingale with respect to this filtration. Then there exists an adapted process $\Gamma(u)$ such that*

$$M(t) = M(0) + \int_0^t \Gamma(u) dW(u), \quad 0 \leq t \leq T \quad (4)$$

Any \mathcal{F} -martingale can be written in the above form. $M(0)$ is an initial condition value and $\int_0^t \Gamma(u) dW(u)$ is an Ito integral (Shreve, 2004). There is only one source of randomness, which is the Wiener process $\{W(t), t \geq 0\}$. We introduce the notion of arbitrage and provide its mathematical characterization. Arbitrage is defined as a strategy with risk-less profit. Formally, arbitrage is defined as portfolio strategy ϕ such that the value process $V_\phi(t)$ satisfies

$$P(V_\phi(T) \geq 0) = 1, \quad P(V_\phi(T) > 0) > 0 \quad (5)$$

In other words, we make no losses with probability 1 and make profit with positive probability. Based on this definition, we state the fundamental theorems of asset pricing. They form the foundation of modern mathematical finance.

Theorem 2 (Fundamental theorem of asset pricing). *If a market model has a risk-neutral probability measure, then it does not admit arbitrage.*

We call the payoff $H \in L^2(P)$ attainable if there is a self-financing strategy $(\phi_0(t), \phi_1(t))$ such that

$$H = V_0 + \int_0^T \phi_1(t) dS(t) + \int_0^T \phi_0(t) dB(t) \quad P-a.s. \quad (6)$$

Equation (6) is also referred to as 'the perfect hedge' (Shreve, 2004). A market model is complete if equation (6) holds for any $H \in L^2(P)$. We reference the following theorem from Shreve (2004).

Theorem 3 (Second fundamental theorem of asset pricing). *In an arbitrage-free market, the model is complete if and only if the equivalent martingale measure P_Q is unique.*

As an example of the market completeness we consider asset $S(t)$ in the Black-Scholes model, which is a martingale under the risk-neutral measure P_Q and satisfies the SDE

$$dS(t) = \sigma S(t) dW(t). \quad (7)$$

Since any contingent claim $H \in L^2(P)$ is supposed to be a Brownian martingale, we can invoke the martingale representation theorem and write

$$H = V(0) + \int_0^T \Gamma(t) dW(t) = V(0) + \int_0^T \frac{\Gamma(t)}{\sigma S(t)} dS(t) = V(0) + \int_0^T \phi(t) dS(t) \quad (8)$$

where $\phi(t) = \frac{\Gamma(t)}{\sigma S(t)}$ is our hedge that makes the claim attainable. The Black-Scholes model is reviewed in detail in section 3.2.1.

2.3 Simplifications compared to real-world case

In this section, we evaluate how much the above assumptions apply to cryptocurrency markets. This passage serves to briefly illustrate how cryptocurrency markets work. In our simplified financial market \mathcal{M} , we rule out any possibility of arbitrage. Furthermore, borrowing and short-selling are permitted. The short-selling assumption is not realistic for cryptocurrency markets. Coinmarketcap ranks 100 largest Cryptocurrency exchanges according to trading volumes (coinmarketcap.com). Among the 50 largest, only Bitfinex, Kraken and Bitmex allow for short-selling. Borrowing is allowed and many exchanges permit margin trading (Makarov et al., 2019). The assumption that \mathcal{M} is arbitrage-free is generally very realistic on financial markets (Cont and Tankov, 2003). Makarov and Schoar (2019) (MK) investigate arbitrage on cryptocurrency markets and observe extensive arbitrage opportunities. Arbitrage spreads hold for short and long time frames ranging from a few hours to a few weeks and are even present when volumes of trades are large (Makarov and Schoar, 2019). Makarov and Schoar (2019) find that especially regional differences between Asian countries and the US offer vast arbitrage opportunities. For a better understanding of cryptocurrency markets, this paper briefly reviews the findings of Makarov and Schoar (2019). They report that transaction costs are not a burden because compared to the arbitrage gains, fixed transaction costs in the Blockchain are neglectable for large trading volumes. In addition, exchanges offer special deals with small costs for "VIP traders" (Makarov et al., 2019). As most exchanges forbid short-selling, it is not possible to benefit from risk-free instantaneous profits by simply short-selling an asset on one exchange and buying it on the other where the asset is traded at lower costs. The trader has to bear some risk to profit from arbitrage (Makarov et al., 2019). One possibility is to hold a positive account of two exchanges and exploit price differences. One would instantaneously sell the higher traded coins and buy additional coins on the cheaper traded exchange. The problem here is that the arbitrageur is exposed to price risk. According to MK, a way to reduce price risk exposure is to borrow coins from *hodlers*, a Bitcoin jargon term for investors who possess coins without the intention to participate in trading (Makarov et al., 2019). The other possibility Makarov and Schoar (2019) identify is through "margin trading". The problem here is "coverage risk" when borrowing coins. Lastly, another risk Makarov and Schoar (2019) identify is "governance risk". When trading on cryptocurrency exchanges, a trader gives his coins to an exchange. The coin is then in the hands of the exchanges. In recent years, large losses resulted from exchange hacks (Makarov et al., 2019).

2.4 Pricing model

This paper assumes that the contingent claim of a cryptocurrency is priced according to the methodology of Hou et al. (2019). The paper suggests the 'Stochastic Volatility with correlated jumps' (SVCJ) option pricing model in the attempt to price CRIX and Bitcoin options. We apply and relate to the conventions and notation in Broadie et al. (2007), Branger et al. (2010), Pan (2002), Eraker et al. (2003) and Belaygorod and Olin (2005) to describe the model. First reviews of the SVCJ

model are conducted by Duffie et al. (2000), Eraker et al. (2003) and Pan (2002). The model allows for stochastic volatility and simultaneous arrivals of jumps in returns and jumps in volatility. Under the physical measure P , the dynamics of asset price $S(t)$ and the latent variance $V(t)$ evolve through

$$\begin{aligned} dS(t) &= (r + \gamma(t)) S(t)dt + \sqrt{V(t)}S(t)dW^s(t) + (e^\xi - 1) S(t)dN(t) - \bar{\mu}_s \lambda S(t)dt \\ dV(t) &= \kappa (\theta - V(t)) dt + \sqrt{V(t)}\sigma_V \left(\rho dW^s(t) + \sqrt{1 - \rho^2} dW^v(t) \right) + Z^v(t)dN(t) \end{aligned} \quad (9)$$

where $\{W^s(t), t \geq 0\}$ and $\{W^v(t), t \geq 0\}$ denote two independent standard Wiener processes and $W(t) = \rho W^s(t) + \sqrt{1 - \rho^2} W^v(t)$ represents a Wiener process $\{W(t), t \geq 0\}$ correlated to $\{W^s(t), t \geq 0\}$ with the correlation coefficient ρ , that is, $E[dW^s(t)dW^v(t)] = \rho dt$. θ is the mean-reversion level, κ the mean-reversion rate, r is the deterministic constant interest rate and σ_V is the volatility of the variance process $V(t)$, commonly referred to as the volatility of the volatility. In the context of hedging options of decentralized cryptocurrencies, we exclude the existence of dividend payments in equation (9). $\{N(t), t \geq 0\}$ is a Poisson process with constant intensity λ . In equation (9), jumps sizes are nonrandom and jumps in volatility and jumps in the asset price are governed by one Poisson process $N(t) = N^s(t) = N^v(t)$. Concurrent jump arrivals permit correlation in jumps sizes (Eraker, 2004). Jump sizes in volatility are assumed to be exponentially distributed $Z^v(t) \sim \varepsilon(\mu_v)$ and conditional on these jumps in latent volatility, jumps in asset prices are conditionally normally distributed with $\xi \stackrel{def}{=} Z^s(t)|Z^v(t) \sim N(\mu_s + \rho_j Z^v(t), \sigma_s^2)$. The mean jump size in the asset price is

$$\bar{\mu}_s = \frac{\exp\left\{\mu_s + \frac{(\sigma_s)^2}{2}\right\}}{1 - \rho_j \mu_v} - 1$$

ρ_j is the correlation coefficient between jumps. In theory, it is reasonable to assume that ρ_j is negative, as large market moves in asset prices coincide with big jump amplitudes in volatility (Broadie et al., 2007). The term $-\bar{\mu}_s \lambda S(t)dt$ is the jump compensator term. The remainder $\gamma(t)$ is the 'total equity premium' (Broadie et al., 2007; Branger et al., 2012). It can be decomposed into

$$\gamma(t) = \eta_s V(t) + \lambda \bar{\mu}_s - \lambda^{\mathbb{Q}} \bar{\mu}_s^{\mathbb{Q}} \quad (10)$$

where $\eta_s V(t)$ represents the 'volatility diffusion risk premium', η_s is the risk premium from volatility and $\lambda \bar{\mu}_s - \lambda^{\mathbb{Q}} \bar{\mu}_s^{\mathbb{Q}}$ the jump risk premium (Branger et al., 2012). $\lambda^{\mathbb{Q}} \bar{\mu}_s^{\mathbb{Q}}$ is described below.

2.4.1 Market incompleteness

In section 2.2, we demonstrate the completeness of the Black-Scholes model (7). The dynamics of the underlying asset price process $S(t)$ described by equation (9) includes jump and stochastic volatility components. Conceding the possibility of the jumps in the asset price $S(t)$ or the introduction of a stochastic component in the variance process $V(t)$ may both individually disrupt the completeness of a given model. For example, in case of the stochastic volatility, a simple argument can show that we can perform a change of measure that would affect the law of $V(t)$ without affecting the martingality of $S(t)$. This is in contradiction with the second fundamental theorem of asset pricing. In conclusion, the model under consideration (9) is not a complete market model.

2.4.2 Option pricing

In section 2.2, we introduce the concept of risk-neutral pricing. The payoff of plain vanilla European option with strike K and maturity T is $(S(T) - K)^+ = \max\{0, S(T) - K\}$. Options are priced under P_Q . Accordingly, $C_t = E_Q \left[e^{-r(T-t)} (S(T) - K)^+ | \mathcal{F}_t \right]$. A change of measure is required to express (9) under risk-neutral measure P_Q . The change of measure in the model under consideration is shown in Duffie et al. (2000) and Pan (2002) is reviewed in detail in Belaygorod and Olin (2005). We review the stochastic differential equation under P_Q . All proofs and calculations are very clearly expressed in Belaygorod and Olin (2005). We choose to review according to the notation in Eraker (2004). Under the risk-neutral measure P_Q , the dynamics of $S(t)$ and $V(t)$ are

$$\begin{aligned} dS(t) &= rS(t)dt + \sqrt{V(t)}S(t)dW(Q)_t^S + (e^\xi - 1)S(t)dN(t) - \bar{\mu}^Q \lambda_S S(t)dt \\ dV(t) &= (\kappa(\theta - V_t) + \eta_v V_t)dt + \sqrt{V(t)}\sigma_V \left(\rho dW(t)^{S,Q} + \sqrt{1 - \rho^2} dW(Q)_t^V \right) + Z^v(t)dN(t) \end{aligned} \quad (11)$$

η^v is the volatility risk premium and η^s is the asset risk premium (Branger et al., 2012) such that $\kappa^Q = \kappa^P + \eta_v$ is the mean reversion speed under the risk-neutral measure and $\kappa^Q \theta^Q = \kappa \theta$ is the mean-reversion level under P_Q . Based on the findings of Pan (2002), Eraker (2004) and Broadie et al. (2007), we assume that $\lambda^Q = \lambda$ and $\sigma_s = \sigma_s^Q$. In other words, the jump-related components are the same under P and P_Q . The drift component is expressed as $dW(Q)_t^i = \eta^i dt + dW(t)^i$, $i = \{s, v\}$ and results from a change of measure by applying the Girsanov (1960) theorem (Belaygorod and Olin, 2005). Follow the conventions of Branger et al. (2010) and Broadie et al. (2007), we assume that $\rho_j^Q = 0$. Since a market where options are traded is non-existent, Hou et al. (2019) choose to set $\eta^v = \eta^s = 0$. Hence, (11) is equivalent to (9) in our setup. In other words, Hou et al. (2019) price options under P .

The *greeks* are sensitivities of an option to changes in underlying parameters on which the value of the option depends (Franke et al. (2015), 2016). This study considers market risk related greeks as investigated in Kurpiel and Roncalli (1999). The following are Δ , Γ , and \mathcal{V} (vega). We will briefly review these greeks. For a more detailed perspective and other greeks such as greeks of higher order, the reader is encouraged to seek for further detailed information in Franke et al. (2015), Hull (2006) and Marroni and Perdomo (2013). In equation (12), Δ is the sensitivity of the option to changes in the underlying, Γ is the sensitivity of the option to changes in Δ and \mathcal{V} is the sensitivity of the option to changes in volatility.

$$\begin{aligned} \Delta &= \frac{\partial C}{\partial S} \\ \Gamma &= \frac{\partial^2 C}{\partial^2 S} \\ \mathcal{V} &= \frac{\partial C}{\partial \sigma} \end{aligned} \quad (12)$$

Δ -hedging eliminates risk from changes in the underlying and requires only one instrument, namely the underlying itself. Γ -neutrality and \mathcal{V} -neutrality require additionally traded options as hedging instruments.

Based on the concepts and principles introduced in section 2.2, the value of the call option at time t

is

$$C_t = E_Q \left[e^{-r(T-t)} (S(T) - K)^+ \right] \quad (13)$$

In this study, option prices are estimated according to the methodology applied in Hou et al. (2019). The option is priced with Monte Carlo Option pricing by Boyle (1977). This method provides an unbiased estimator of the option price. The review of the theoretical concept is mainly based on Glasserman (2004). Let C denote the unknown option price. We generate n paths of $S(t)$ under the risk neutral measure P_Q . The discounted terminal payoff at each path is $C_i = e^{-rT} (S(T) - K)^+, i = 1 \dots n$. We consider the point estimator of the unknown option price C

$$\hat{C}_n = e^{-rT} \frac{1}{n} \sum_{i=1}^n (S_i(T) - K)^+ \quad (14)$$

This point estimator \hat{C}_n is an unbiased estimator of C

$$E[\hat{C}_n] = E \left[e^{-rT} \frac{1}{n} \sum_{i=1}^n (S_i(T) - K)^+ \right] = E[e^{-rT} (S(T) - K)^+] = C \quad (15)$$

The unbiased estimated standard deviation of the sample C_1, \dots, C_n is

$$\hat{\sigma}_c = \sqrt{\frac{1}{n-1} \sum_{i=1}^n (C_i - \hat{C}_n)^2} \quad (16)$$

According to the strong law of large numbers, this estimator is strongly consistent $\hat{C}_n \xrightarrow{a.s.} C$. It converges with probability 1 to the true option price C . Finally, the interval estimator of our option price for a confidence level of $1 - \alpha$

$$\left[\hat{C}_n - Z_{1-\frac{\alpha}{2}} \frac{\hat{\sigma}_c}{\sqrt{n}}, \hat{C}_n + Z_{1-\frac{\alpha}{2}} \frac{\hat{\sigma}_c}{\sqrt{n}} \right] \quad (17)$$

where $Z_{1-\frac{\alpha}{2}}$ denotes the $1 - \alpha$ quantile of the standard normal distribution. For further details, the reader is referred to Glasserman (2004).

2.5 Discretization

The computational implementation for simulation purposes requires a discretization of the continuous-time processes with the dynamics described in equation (9). The finite time horizon is partitioned into n time steps of equal distance dt such that $T = \{0, dt, 2dt, \dots, ndt = T\}$. Belaygorod and Olin (2005) state that it is difficult to distinguish whether many small jumps or one larger jump occurred in a short time interval. The discrete partition of the finite time horizon T into n time steps of size dt is not sufficiently granular to enable a clear distinction between the frequency of jump arrivals and the amplitude of jump sizes. For simulation, Belaygorod and Olin (2005) propose to model arrivals of jumps by Bernoulli random variables $J_{dt}^s = J_{dt}^v \sim \text{Ber}(\lambda)$. The Euler-Maruyama method is applied to discretize equation (9). The Euler discretization applied in this paper is

$$\begin{aligned} \frac{S(t+dt) - S(t)}{S(t)} &= (\mu - \bar{\mu}_s \lambda) dt + \sqrt{V(t)dt} X_1 + Z^s(t+dt) J(t+dt) \\ V(t+dt) &= V(t) + \kappa_v (\theta - V(t)) dt + \sigma_V \sqrt{V(t)dt} X_2 + Z^v(t+dt) J(t+dt) \end{aligned} \quad (18)$$


where X_1 and X_2 are two standard normal variables correlated with coefficient ρ . μ is the drift. In equation (9), $\mu = r + \gamma(t)$. Equation 18 presents only one possibility to discretize the solution of equation (9). The procedure with the solution (18) is a less precise method to discretize the solution of equation (9). Another more precise method is to solve equation (9) with Ito calculus for jump processes (Belaygorod and Olin, 2005). For further details, the reader is referred to section 4 in Belaygorod and Olin (2005). Broadie and Kaya (2006) describe an even more exact method for simulating affine jump diffusion processes. Since the scope of this paper is hedging, it is sufficient to apply the representation in equation (18). For different discretization methods, the reader is recommended to look into the book of Kienitz and Wetterau (2013). Hou et al. (2019) also apply the Euler-Maruyama discretization described in Johannes and Polson (2009). They calibrate the drift component with one parameter μ . The calibrated parameters are reviewed in section 2.5.1.

2.5.1 Calibration

According to the concepts in section 2.2, options are priced under the risk-neutral measure P_Q . Therefore, proper calibration requires the estimation of parameters under P_Q . This is not feasible in the case cryptocurrencies, because options are not officially exchange-traded (Hou et al., 2019). Therefore, Hou et al. (2019) calibrate the parameters $\Theta = \{\mu, \mu_s, \sigma_s, \lambda, \alpha, \beta, \sigma_v, \rho, \rho_j, \mu_v\}$, where $\alpha = \kappa\theta$ and μ_s is the average jump size in returns, from returns under the physical measure P . They apply Monte Carlo Markov Chain (MCMC), a Bayesian calibration method initially applied by Eraker et al. (2003), to estimate the parameters of the SVCJ for BTC and CRIX in a time horizon from 31.03.2014 to 29.09.2017. Perez (2018) extends the estimation to more cryptocurrencies until 30.09.2018. The purpose of this paper is to evaluate the hedge performance of options priced by Hou et al. (2019). Therefore, the parameters calibrated by Hou et al. (2019) presented in table 1 are assumed as given.

	μ	μ_y	σ_y	λ	α	β	ρ	σ_v	ρ_j	μ_v
mean	0.042	-0.049	2.061	0.051	0.010	-0.190	0.275	0.007	-0.210	0.709
p-value	0.006	0.371	0.432	0.007	0.001	0.009	0.069	0.001	0.364	0.089

Table 1: SVCJ calibrated parameters of the CRIX from Hou et al. (2019). Red means strong positive significance (below 0.001 %) and blue strong means negative significance (below 0.001 %)

 SVCJ_CRIX

In table 1, λ is small. The interpretation is that jumps are rare. As expected, ρ_j is negative but statistically insignificant. This is in line with the conventions in Broadie et al. (2007) and the findings of Eraker et al. (2003), Eraker (2004) and Chernov et al. (2003). Broadie et al. (2007) outline the difficulties in estimating ρ_j by reason of the fact that jumps occur seldomly. Broadie et al. (2007) and

Branger et al. (2012) recommend to set $\rho_j = 0$. We accept this suggestion and set $\rho_j = 0$. Under this assumption, equation (9) distinguishes itself from the 'Stochastic Volatility with Jumps' (SVJ) model by Bates (1996) by jumps in volatility. In other words, the model includes the additional parameter μ_v . Hou et al. (2019) outline that ρ is positive and significant. This is contrary to what is expected. It is expected that when prices increase, volatility decreases (Broadie et al., 2007). The interpretation of Hou et al. (2019) is an inverse leverage effect. They refer to the finding of Schwartz and Trolled (2009) on commodity markets.

In summary, this paper tries to mimic the behavior of the CRIX in a simulation study where the dynamics of the underlying are described by the SDE in equation (9). Equation (9) is discretized by equation (18) with the above-formulated parameter conventions, where $\rho_j = 0$. We assume that the values of the parameters are the ones listed in table 1. Figure 2 illustrates 25 trajectories of our data-generating process $S(t)$.

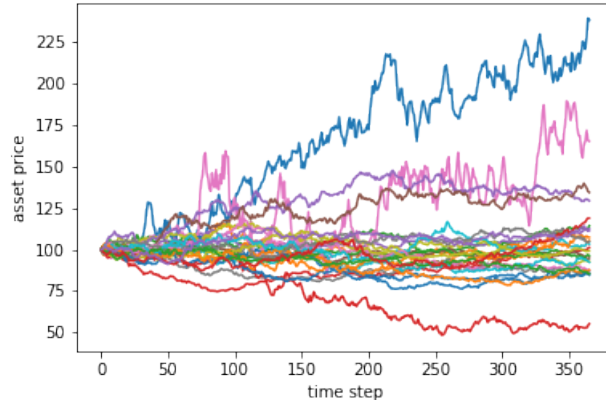


Figure 2: 25 Euler discretized trajectories of $S(t)$ for a time horizon of 1 year

 SVCJ_MC

The trajectories of figure 2 illustrate different scenarios. In equation (9), jumps sizes in returns are

$$Z^s(t)|Z^v(t) \sim N(\mu_s + \rho_j Z^v(t), \sigma_s^2)$$

distributed. Accordingly, jumps sizes can be very large. This is illustrated by the blue and pink trajectory in figure 2. Since λ is fairly small, jumps are rare. For the hedging procedure it is important to evaluate the relevance of these jumps. Figure 3a and 3b illustrate 4000 asset paths of the SVCJ. The purpose of these illustrations is to evaluate the main drivers of our underlying $S(t)$. In figure 3a, jumps are present and $\lambda \neq 0$. For comparison, in figure 3b the parameter λ is set to $\lambda = 0$. In other words, the presence of jumps is excluded. In figure 3a large jumps amplitudes lead to prices rises up to 600 % within 1 year. However, in the majority of the cases paths range roughly up to $S(t) = 250$. This price range corresponds to what is observed in figure 3b. This indicated that the main driver

of the price dynamics are not jumps but stochastic volatility. The discussion about adding jumps is summarized in Broadie et al. (2007). For example, Eraker (2004) finds that adding jumps may lead to a better model fit, yet has a small impact on option pricing. For further information, the reader is referred to Broadie et al. (2007). Hou et al. (2019) report that most studies on cryptocurrencies do not account for jumps. They choose to add jumps to pricing in reference to Scaillet et al. (2018). Scaillet et al. (2018) report that in comparison to "traditional markets", jumps on Cryptocurrency markets tend to occur more frequently. Judging on the movements of the CRIX illustrated in figure 1, this paper believes that jumps should be included to pricing and that the presence of jumps should not be disregarded. Single cases can have extreme amplitudes in jump sizes. The question we ask ourselves is how this impacts the P&L.

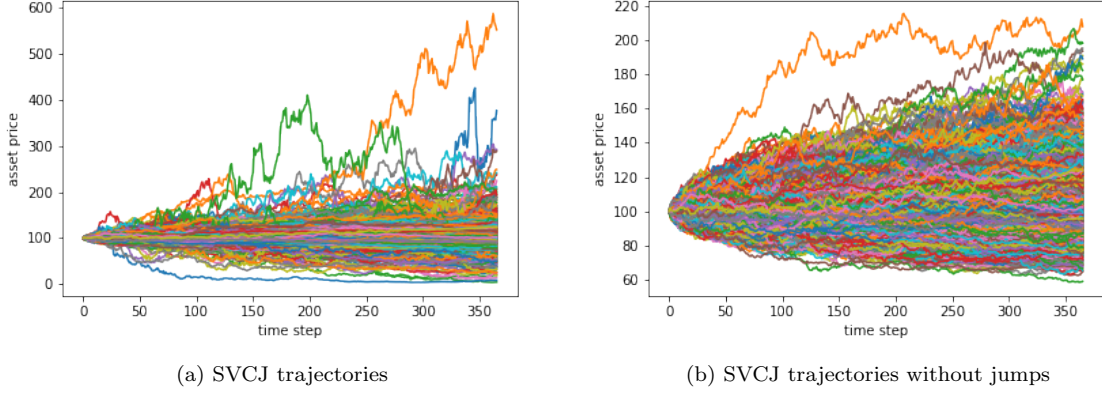


Figure 3: 4000 simulated trajectories of $S(t)$ with jumps in returns and volatility in 3a and without jumps in 3b

 SVCJ_MC

3 Hedging

We have outlined the importance of hedging in terms of mitigation of risk and a deeper understanding of the market. In section 2.4.1 we address market incompleteness. There is no perfect replication (6). Thus, we face the trade-off between selecting a simpler and preferably complete market model or choosing alternative hedging strategies (Packham and Detering, 2016). A "conservative approach" (Cont and Tankov, 2003) is to almost surely hedge all risk associated with the contingent claim

$$\mathbb{P} \left(V_\phi(t) = V(0) + \int_0^t \phi dS \geq H \right) = 1 \quad (19)$$

We review the explanation of superhedging in Cont and Tankov (2003). If the strategy is self-financing, the costs of superhedging correspond to $V_\phi(0)$. Superhedging is neither desirable nor a very efficient strategy that hedges against large price movements resulting from, for example, jump amplitudes. To

demonstrate the inadequacy of this strategy in our investigation, it is sufficient to state that investors and financial institutions enter markets willing to bear some risk because the risk is rewarded. It is hardly the case that someone would participate in a market like a cryptocurrency market and to hedge all risk associated with this market.

A third way to go is utility-based hedging. We choose a hybrid method. We hedge under model misspecification, yet two of our models are incomplete market models such that we also apply quadratic hedging.

3.1 Hedging in discrete time

For the empirical implementation in discrete time, the finite time horizon T is partitioned into $T = \{0, dt, 2dt, \dots, ndt = T\}$. The hedging instruments are the underlying $S(t)$ and the money market account $M(t)$, precisely, a risk-free asset $B(t), t \geq 0$ with $B(0) = 1$. Our strategy ϕ is a self-financed strategy as defined in equation (2).

At time $t_0 = 0$ and $B(0) = 1$, the value of the portfolio is

$$\begin{aligned} V_\phi(0) &= C_{SV CJ}(0, S(0)) = \phi(0)S(0) + (C_{SV CJ}(0, S(0)) - \phi(0)S(0))B(0) \\ M(0) &= C_{SV CJ}(0, S(0)) - \phi(0)S(0) \end{aligned} \quad (20)$$

At time $t \geq 0$, the value of the portfolio is

$$\begin{aligned} M(t) &= M(t - dt) + (\phi(t - dt) - \phi(t)) \frac{S(t)}{B(t)} \\ V(t) &= \phi(t - dt)S(t) + M(t - dt)B(t - dt)e^{r dt} = \phi(t)S(t) + \underbrace{\frac{V(t) - \phi(t)S(t)}{B(t)}}_{=M(t)} B(t) \end{aligned} \quad (21)$$

At maturity T , the final position is

$$V(T) = \phi(T - dt)S(t) + M(T - dt)B(t) \quad (22)$$

At maturity, the profit is $V_T - \max\{(S(t) - K)^+, 0\}$. We will implement this strategy in the delta hedge.

3.2 Hedge models

In this section, we briefly review the main properties of our hedge models.

3.2.1 Black-Scholes asset pricing model

We start with the 'classic Black-Scholes' option pricing model by Black and Scholes (1973). The Black-Scholes model is particularly popular because of the Black-Scholes formula, a closed-form solution of the option price. This makes it popular among practitioners, as it provides a quick initial evaluation of option prices (Green, 1999). The dynamics of the asset price $S(t)$ under the physical measure \mathbb{P} are described by the SDE

$$dS(t) = \mu S(t)dt + \sigma S(t)dW(t) \quad (23)$$

$\{W(t), t > 0\}$ denotes a standard Wiener process, μ is the drift and σ referred to as the *volatility*, the standard deviation around the drift. As already stated in section 2.2, options are priced and calibrated under the risk-neutral measure P_Q . Under this measure, the dynamics of the $S(t)$ are described by the stochastic differential equation

$$dS(t) = rS(t)dt + \sigma S(t)dW(t) \quad (24)$$

In reference to the Girsanov (1960) theorem for a change of measure from P to P_Q , the reader is referred to Shreve (2004) or Jeanblanc (2009) for a detailed review. The price of a European call at time t written on the underlying $S(t)$, with strike K and time-to-maturity τ is

$$C(S(t), \tau) = S(t)\Phi(y + \sigma\sqrt{\tau}) - e^{-r\tau}K\Phi(y) \\ y = \frac{\log \frac{S(t)}{K} + \left(r - \frac{\sigma^2}{2}\right)\tau}{\sigma\sqrt{\tau}} \quad (25)$$

where $\Phi(x)$ is the cumulative distribution function (CDF) of a standard normal random variable and r is the risk-neutral rate. The Δ of equation (25) is

$$\Delta_{BS}(S(t), t) = \frac{\partial C}{\partial S} = \Phi(y + \sigma\sqrt{\tau}) \quad (26)$$

According too the properties of the CDF, $\Delta_{BS}(S(t), t)$ is bounded between 0 and 1. Γ of the option is given by

$$\Gamma_{BS}(S(t), t) = \frac{1}{\sigma S\sqrt{\tau}}\varphi(y + \sigma\sqrt{\tau}) \quad (27)$$

In equation (23) and equation (25), σ is assumed to be constant. Returns are log-normally distributed. These assumptions are limitations of the BS model. Constant volatility is empirically not supported (Heston, 1993). The notion *implied volatility* refers to the volatility implied by the Black-Scholes formula presented in equation (25) on market prices C_{market} of options. The implied volatility σ_{iv} solves

$$S\Phi(y + \sigma_{iv}\sqrt{\tau}) - e^{-r\tau}K\Phi(y) = C_{market} \quad (28)$$

The sensitivity of the option prices computed with equation (25) to changes in volatility is denoted by \mathcal{V} and is referred to as the *vega* of an option. The \mathcal{V} is presented in equation (29).

$$\mathcal{V}_{BS}(S(t), t) = S\sqrt{\tau}\varphi(y + \sigma\sqrt{\tau}) \quad (29)$$

Hedging Δ eliminates the risk from changes in the underlying $S(t)$, hedging Γ eliminates the risk from changes in Δ and hedging \mathcal{V} eliminates the risk from changes in volatility (Franke et. al, 2015).

The Black-Scholes model is the simplest misspecified model under consideration. It is a special case of the dynamics described in equation (9). Jumps are excluded $N^s(t) = N^v(t) = 0, \forall t \in [0, T]$ and volatility is assumed to be constant $V(t) = \sigma_v = 0$. We list a few reasons to justify the choice of this clearly misspecified hedge model. In section 2.2, we briefly demonstrate the completeness of this market model. The motivation behind the choice of a misspecified complete market hedge models is the existence of a replicating strategy (Packham and Detlefsen, 2016). Regardless of its limitations,

this 'classic' Black-Scholes model remains highly popular among practitioners (El Karoui et al., 1998, Bergomi, 2015). El Karoui et al. (1998) show the conditions under which the Black-Scholes option pricing model is robust for hedging. The following briefly derives the hedge error in the Black-Scholes model. It is mainly based on Bergomi (2015). In alliance with section 3.1, we take an option writer's perspective. The option writer shorts the call C , longs the asset S and the remainder goes to the money market account for which holds $dB_t = rB_t dt$. The value of this portfolio in t is

$$V_\phi(t) = -C(t) + \Delta(t)S(t) + \frac{(C(t) - \Delta(t)S(t))}{B_t} B_t \quad (30)$$

We have already demonstrated that this position is self-financing. Accordingly,

$$dV_\phi(t) = -dC(t) + \Delta(t)dS(t) + (C(t) - \Delta(t)S(t))rdt \quad (31)$$

We now apply Ito's lemma to equation (25)

$$dC(t) = \frac{\partial C}{\partial t} dt + \frac{\partial C}{\partial S} dS(t) + \frac{1}{2} \frac{\partial^2 C}{\partial S^2} \langle dS(t) \rangle \quad (32)$$

According to the definitions of the greeks in equation (12), we express equation (32) in terms of the sensitivities

$$dC(t) = \frac{\partial C}{\partial t} dt + \Delta(t)dS(t) + \frac{1}{2}\Gamma(t)\langle dS(t) \rangle \quad (33)$$

Accordingly,

$$dV_\phi(t) = \left(-\frac{\partial C}{\partial t} dt - rS(t)\Delta(t) + rC(t) \right) dt - \frac{1}{2}\Gamma(t)\langle dS(t) \rangle \quad (34)$$

We want to add and subtract $\frac{1}{2}\sigma^2 S^2 \frac{\partial^2 C}{\partial S^2}$ in equation (34) and use Black-Scholes partial differential equation

$$\frac{\partial C}{\partial t} + \frac{1}{2}\sigma^2 S^2 \frac{\partial^2 C}{\partial S^2} + rS \frac{\partial C}{\partial S} - rC = 0 \quad (35)$$

to obtain the resulting hedge error

$$\begin{aligned} dV_\phi(t) &= \frac{1}{2}\Gamma S(t)^2 \sigma^2 dt - \frac{1}{2}\Gamma \langle dS(t) \rangle \\ &= \frac{1}{2}\Gamma S(t)^2 (\sigma^2 - \hat{\sigma}^2(t)) dt \end{aligned} \quad (36)$$

where $\hat{\sigma}^2(t)$ denotes the realized volatility at time t . $\hat{\sigma}$ that depends on the market and σ is model-dependent. The P&L from this position is

$$P\&L(t) = \int_0^T e^{-r(T-t)} \frac{1}{2}\Gamma S(t)^2 (\sigma^2 - \hat{\sigma}^2(t)) dt \quad (37)$$

Γ depends on the claim and determines the convexity of the option. If $\Gamma(t) > 0$ and $\hat{\sigma}^2(t) \geq \sigma^2$, the strategy is a superhedge.

3.2.2 Heston stochastic volatility model

Non-deterministic fluctuations in historic volatility set the ground to assume that volatility could be potentially stochastic (Kienitz et al., 2013). Heston (1993) proposes an extension to the Black-Scholes option-pricing model presented in section 3.2.1. In the Heston (1993) Stochastic Volatility model the dynamics of the asset price process $S(t)$ and the latent volatility process $V(t)$ are

$$\begin{aligned}\frac{dS(t)}{S(t)} &= \mu dt + \sqrt{V(t)} dW^s(t) \\ dV(t) &= \kappa (\theta - V(t)) dt + \sigma \sqrt{V(t)} \left(\rho dW^s(t) + \sqrt{1 - \rho^2} dW^v(t) \right) \\ S(0) &= S_0 \\ V(0) &= V_0\end{aligned}\tag{38}$$

where $W^v(t)$ and $W^s(t)$ are two independent standard Wiener processes as in equation (9) and $W(t) = \rho W^s(t) + \sqrt{1 - \rho^2} W^v(t)$ represents a Wiener process $\{W(t), t \geq 0\}$ correlated to $\{W^s(t), t \geq 0\}$ with correlation ρ . θ is the long-term variance or mean reversion level, κ is the mean reversion speed and σ_v is the volatility of the volatility of the variance process $V(t)$. In current literature such as Bergomi (2015) or Shreve (2004) σ_v is predominantly referred to the volatility of volatility. The drift term $\kappa (\theta - V(t))$ of the latent volatility process is mean-reverting around its long term mean θ . This means that the drift term is negative for $\theta > V(t)$ and otherwise positive. If the Feller condition $2\kappa\theta > \lambda$ holds, this process is positive with probability 1. The Heston (1993) model is an affine process and the special case of the dynamics of the underlying described by equation (9), where we rule out the existence of jumps, precisely $\lambda = 0$ and $N^s(t) = N^v(t) = 0, \forall t \in [0, T]$. Due to this affine specification Heston (1993) model has a closed-form solution that resembles the 'classic' Black-Scholes formula equation (25). Bergomi (2015) argues that this is potentially one of the reasons why this particular model more popular than other stochastic volatility models among practitioners. Heston (1993) derives the closed-form solution of a European call option

$$\begin{aligned}C(S_0, K, V_0, t, T) &= SP_1 - Ke^{-(r)(T-t)} P_2 \\ P_j &= \frac{1}{2} + \frac{1}{\pi} \int_0^\infty \text{Re} \left[\frac{e^{-iu \ln K} \varphi_j(S_0, V_0, t, T, u)}{iu} \right] du, \quad j = 1, 2 \\ \varphi_j(S_0, V_0, \tau; \phi) &= \exp \{C_j(\tau; \phi) + D_j(\tau; \phi) V_0 + i\phi S_0\} \\ C(\tau, \phi) &= (r - q)\phi i\tau + \frac{\kappa\theta}{\sigma^2} \left\{ (b_j - \rho\sigma\phi i + d)\tau - 2 \ln \left[\frac{1 - ge^{d\tau}}{1 - g} \right] \right\} \\ D(\tau; \phi) &= \frac{b_j - \rho\sigma\phi i + d}{\sigma^2} \left[\frac{1 - e^{d\tau}}{1 - ge^{d\tau}} \right] \\ g &= \frac{b_j - \rho\sigma\phi i + d}{b_j - \rho\sigma\phi i - d} \\ d &= \sqrt{(\rho\sigma\phi i - b_j)^2 - \sigma^2 (2u_j\phi i - \phi^2)}\end{aligned}\tag{39}$$

where φ_1, φ_2 are the characteristic functions of interest with $u_1 = 0.5$, $u_2 = -0.5$, $a = \kappa\theta$, $b_1 = \kappa + \lambda - \rho\sigma$ and $b_2 = \kappa + \lambda$. The closed-form solution of the option price as presented in equation (39) enables to analytically express the Greeks of the option. In the case of the Heston model, we consider

Δ_{SV} and the \mathcal{V}_{SV} as relevant sensitivities for hedging purposes. The delta Δ_{SV} of the Heston model is

$$\begin{aligned}\Delta_{SV} &= \frac{\partial C}{\partial S} = P_1 + S \frac{\partial P_1}{\partial S} - K \frac{\partial P_2}{\partial S} \\ &= P_1 + \frac{S}{\pi} \int_0^\infty \operatorname{Re} \left\{ \frac{e^{-i\varphi \ln K} f_1(x, v, \tau; \varphi)}{S} \right\} d\varphi - \frac{K}{\pi} \int_0^\infty \operatorname{Re} \left\{ \frac{e^{-i\varphi \ln K} f_2(x, v, \tau; \varphi)}{S} \right\} d\varphi\end{aligned}\quad (40)$$

\mathcal{V}_{SV} is the sensitivity of $C_{heston}(S(t), t)$ expressed by equation (39) to changes in the volatility of the volatility σ_v

$$\begin{aligned}\mathcal{V}_{SV} &= \frac{\partial C(S, t)}{\partial \sigma} = S \frac{\partial P_1}{\partial \sigma} - K \frac{\partial P_2}{\partial \sigma} \\ \frac{\partial P_i}{\partial \sigma} &= \frac{1}{\pi} \int_0^\infty \operatorname{Re} \left\{ \frac{e^{-i\varphi \ln K} f_i(x, v, \tau; \varphi)}{i\varphi} \cdot D_j(\tau; \varphi) \right\} d\varphi, \quad i = \{1, 2\}\end{aligned}\quad (41)$$

Stochastic volatility is an additional source of randomness. In section 2.4.1, we mention the market incompleteness and wish to investigate the impact on hedging. Kurpiel and Roncalli (1999) study the hedge performance of first- and second order greeks. This study will consider the delta-, delta-vega, and the minimum variance hedge for the Heston (1993) model. We will review the strategies and perform an empirical simulation study on delta-hedging. The following overview is mainly based on Albrecher et al. (2013). We hedge the sensitivity to changes in the underlying $S(t)$ with the underlying itself and the money market account $M(t)$. At time $t_0 = 0$ the value of the portfolio is

$$V_\phi(0) = C_0(0, t_0) = \Delta_{SV} S(0) + (C(S, V, t) - \Delta_{SV} S(0)) \quad (42)$$

At time t , the changes in the portfolio are

$$dV_\phi(t) = \Delta_{SV} dS + (C(S, V, t) - \Delta_{SV} S(t)) r dt - dC(S, V, t) \quad (43)$$

In analogous manner to the previous case, we apply Ito's lemma to obtain under a risk-neutral measure

$$\begin{aligned}dC(S, V, t) &= \left(\frac{\partial C}{\partial S} r S + \frac{\partial C}{\partial V} \kappa(\theta - V) + \frac{\partial C}{\partial t} + \frac{1}{2} \frac{\partial^2 C}{\partial S^2} V S^2 + \frac{1}{2} \frac{\partial^2 C}{\partial V^2} \sigma^2 V + \frac{\partial^2 C}{\partial V \partial S} \rho V \sigma S \right) dt \\ &\quad + \frac{\partial C}{\partial S} \sqrt{V} S dW(t) + \frac{\partial C}{\partial V} \sigma \sqrt{V} d\tilde{W}_t\end{aligned}\quad (44)$$

The changes in the portfolio are

$$\begin{aligned}dV_\phi(t) &= \left(-\frac{\partial C}{\partial S} \right) dS + \Delta_{SV} dS - \frac{\partial C}{\partial V} dV + (C(S, V, t) - \Delta_{SV} S(t)) r dt \\ &\quad - \left(\frac{\partial C}{\partial t} + \frac{1}{2} \frac{\partial^2 C}{\partial S^2} V S^2 + \frac{1}{2} \frac{\partial^2 C}{\partial V^2} \sigma^2 V + \frac{\partial^2 C}{\partial V \partial S} \rho V \sigma S \right) dt\end{aligned}\quad (45)$$

Delta hedging, that is, $\Delta_{SV} = \frac{\partial C}{\partial S}$ eliminates the sensitivity to changes in the asset price. In equation (45), delta hedging does not eliminate the risk from stochastic volatility. The solution to this problem is to complete the market with one additionally liquid option written on the same underlying $S(t)$ and to perform a *delta-vega* hedging. Albrecher et al. (2013) recommend to take the same option type with a longer maturity or a different strike. The option writer shorts the call option C and takes the position Δ in the asset and Λ in the second contingent claim. The following illustrations are from Albrecher et al. (2013). The value of the portfolio at time t is

$$V_\phi(t) = -C(t) + \Lambda C_2(t) + \Delta S(t) \quad (46)$$

and the corresponding change is

$$dV_\phi(t) = \Delta dS + (C(S, V, t) - \Delta S(t) - \Lambda C_2(S, V, t)) r dt - dC(S, V, t) + \Lambda dC_2(S, V, t) \quad (47)$$

That is

$$\begin{aligned} dV_\phi(t) &= (C(S, V, t) - \Delta S(t) - \Lambda C_2(S, V, t)) r dt \\ &\quad - \left(\frac{\partial C}{\partial t} + \frac{1}{2} \frac{\partial^2 C}{\partial S^2} V S^2 + \frac{1}{2} \frac{\partial^2 C}{\partial V^2} V + \frac{\partial^2 C}{\partial V \partial S} \rho V S \right) dt \\ &\quad + \Lambda \left(\frac{\partial C_2}{\partial t} + \frac{1}{2} \frac{\partial^2 C_2}{\partial S^2} V S^2 + \frac{1}{2} \frac{\partial^2 C_2}{\partial V^2} V + \frac{\partial^2 C_2}{\partial V \partial S} \rho V S \right) dt \\ &\quad + \left(\Lambda \frac{\partial C_2}{\partial S} - \frac{\partial C}{\partial S} + \Delta \right) dS + \left(\Lambda \frac{\partial C_2}{\partial V} - \frac{\partial C}{\partial V} \right) dV \end{aligned} \quad (48)$$

Setting $\Lambda = \frac{\partial C / \partial v}{\partial C_2 / \partial v}$ and $\Delta = \frac{\partial C}{\partial S} - \Lambda \frac{\partial C_2}{\partial S}$ removes all sources of randomness. In other words, the portfolio is risk-free.

3.2.3 Merton Jump diffusion model

According to the findings of Scaillet et al. (2018), there is evidence for jumps in cryptocurrency markets. The third and final hedge model under consideration is the jump diffusion model by Merton (1976). Merton (1976) extends equation (23) to

$$\frac{dS(t)}{S_{t-}} = (\mu - \kappa \lambda) dt + \sigma dW(t) + (J(t) - 1) dN_t \quad (49)$$

where μ denotes drift, $\{W(t), t > 0\}$ denotes a standard Wiener process and σ is the volatility during ordinary times. $J(t) = \sum_{j=1}^{N(t)} (Y_j - 1)$ represents a compound Poisson process, where $\{N(t), t > 0\}$ is a homogeneous Poisson process with intensity $\lambda > 0$ and Y_i denotes the i.i.d. jump sizes independent of $N(t)$ and $W(t)$. The Merton (1976) model assumes that that jump sizes are $\log Y_i \sim N(m, \delta^2)$ distributed. Lastly, $\kappa = E[Y_i - 1] = \exp\left[m + \frac{\delta^2}{2}\right] - 1$ is chosen such that the compensator term makes $M(t) \stackrel{def}{=} J(t) - \kappa \lambda t$ a martingale (Shreve, 2004). In section 2.4.1, we have already stated that models with jumps are incomplete market models. The martingale measure P_Q is not unique.

Merton assumes that jumps are diversifiable. Therefore, a change of measure is only applied to the drift component in equation (49). The key idea is to choose find an expression of μ_{P^*} such that $\hat{S}(t) = S(t)e^{-rt}$ is a martingale. This is the case for

$$\mu_{P^*} = r - \frac{\sigma^2}{2} - \lambda E[Y_i - 1] = r - \frac{\sigma^2}{2} - \lambda \left[\exp\left(m + \frac{\delta^2}{2}\right) - 1 \right]$$

such that the asset price under the risk neutral measure is

$$S(t) = S(0) \exp \left[\mu_{P^*} t + \sigma W_{P^*}(t) + \sum_{i=1}^{N_t} Y_i \right] \quad (50)$$

This is not a very realistic assumption. With this logic, a diversified representative such as the S&P 500 index would than not include any jumps (Cont and Tankov, 2003). Figure 1 indicates that this is

certainly not the case for the CRIX, because jump amplitudes are very large.

Merton derives the closed-form solution of the option price C_{Merton}

$$C_{Merton}(S(t), t) = \sum_{i=0}^{\infty} \frac{\exp(-\bar{\lambda}\tau)(\bar{\lambda}\tau)^i}{i!} C_{BS}(S(t), \tau, \sigma_i, r_i) \quad (51)$$

where $C_{BS}(S(t), \tau, \sigma_i, r_i)$ is price of a call option under Black-Scholes as presented in equation (25). Furthermore, $\bar{\lambda} = \lambda(1 + \kappa)$, $\sigma_i = \sigma^2 + \frac{i\sigma^2}{\tau}$ and $r_i = r - \kappa\lambda + i\frac{\log(1+\kappa)}{\tau}$. Given this closed-form solution in equation (51), the delta in the Merton jump diffusion option pricing model is

$$\Delta_{Merton}(S(t), t) = \frac{\partial C_{Merton}(S(t), t)}{\partial S(t)} = \sum_{i=0}^{\infty} \frac{\exp(-\bar{\lambda}\tau)(\bar{\lambda}\tau)^i}{i!} \Delta_{BS}(S(t), \tau, \sigma_i, r_i) \quad (52)$$

The Merton (1976) jump diffusion model is also a special case of the SVCJ. For a constant volatility component $V_t = \theta$ and no jumps in volatility $Z^v(t) = 0$ and $\sigma_V = 0$ the dynamics of the general model in equation (9) correspond to equation (49). This model is misspecified in terms of volatility, jumps in volatility and jump size distribution. The idea behind the choice of this model is related to the terminology of what we believe a trader would do. In the evidence of discontinuities from jumps, a trader would switch from the Black-Scholes model to a more sophisticated model that includes jumps.

3.3 Quadratic hedging

Lastly, we observe quadratic hedging. The quadratic hedging provides variance-related hedging measures. For a contingent claim $H \in L^2(P)$ we consider the cost process

$$C_\phi(t) = H - \int_0^t \phi(u) dS(u). \quad (53)$$

Föllmer and Sondermann (1986) define a remaining risk as a measure of uncertainty at time t as

$$R_\phi(t) = \mathbb{E} \left[(C_\phi(T) - C_\phi(t))^2 | \mathcal{F}_t \right] \quad (54)$$

The portfolio strategy ϕ is a risk-minimizing strategy at time t if for all $\tilde{\phi}$ such that $\phi(s) = \tilde{\phi}(s)$ for all $0 < s < t$ holds

$$R_\phi(t) \leq R_{\tilde{\phi}}(t) \quad \mathbb{P} - \text{a.s. for every } t \in [0, T]. \quad (55)$$

Under the assumption of symmetric losses and gains, the aim is to find the strategy $\phi(t)$ that minimizes the hedging error in terms of the mean-squared error. Under the risk neutral measure, we aim to minimize the following expectation

$$(V(0), \phi^*(t)) = \underset{V(0), \phi(t)}{\operatorname{argmin}} \mathbb{E}_Q \left[\left(C_T - V(0) - \int_0^T \phi(u) dS(u) \right)^2 \right] \quad (56)$$

A procedure for the derivation of these strategies is provided in Cont and Tankov (2003) and Kienitz and Wetterau (2013). The basic idea is to apply a decomposition such that we get a hedgeable and

an unhedgeable component. The risk-minimizing strategy for the Heston model is

$$\phi_{min}^* = \frac{\partial C(S, v, t, T)}{\partial S} + \rho \sigma \frac{\partial C(S, v, t, T)}{\partial v} \frac{1}{S(t)}$$

For further details, the reader is referred to Poulsen et al. (2009).

The derivation in the case of Merton is provided in Cont and Tankov (2003)

$$\phi_{min}^* = \frac{\sigma^2 \frac{\partial C(t)}{\partial S(t)} + \frac{1}{S(t)} \int_{-\infty}^{\infty} (e^z - 1) (C_t(S(t)e^z) - C(S(t))) \nu(dz)}{\sigma^2 + \int_{-\infty}^{\infty} (e^z - 1) \nu(dz)} \quad (57)$$

where ν comes from the Levy-Khintchine triplet of the process S_t .

The hedge error under consideration is the one reported in Poulsen et al. (2009)

$$\text{hedge error} = 100 \times \frac{\sqrt{\text{Var}^P(\text{Cost}(T))}}{e^{-rT} \mathbb{E}^{\min}([S(T) - K]^+)} \quad (58)$$

This paper's interpretation of the hedge error is the following: the standard deviation can be interpreted as a measure of uncertainty. The scope of risk is to mitigate uncertainties.

3.4 Hedge model calibration

According to the findings of Green and Figlewski (1999), Sun et al. (2015) and El Karoui et al. (1998), the hedge model calibration vastly impacts the performance of the hedge models. In this particular setup, we lack historic option prices, as there is no market for cryptocurrency options. In reference to section 2.4.2, we assume the parameters from table 1 as given and price contingent claims with Monte Carlo simulation. On the basis of the simulated option prices presented in table 2, table 12 and table 13, we calibrate the parameters of the hedge models. Carr and Madan (1999) introduce option pricing based on Fast Fourier transform (FFT). Borak et al. (2005) illustrate "FFT based option pricing" for the Heston (1993) model, Merton (1976) jump diffusion model and the SVJ model by Bates (1996). The theoretical review of the methodology and computational implementation is based on Cizek et al. (2011), Poklewski-Koziell (2012) Hilpisch (2015) and Kienitz and Wetterau (2013). According to the concepts of arbitrage theory in section 2.2, the present value of the European call option at $t = 0$ is

$$C_0 = \mathbb{E}_{P_Q} [e^{-rT} C_T] = e^{-rT} \int_k^{\infty} (e^s - e^k) q_T(s) ds \quad (59)$$

where $q_T(s)$ denotes the density of the log-price of the underlying $s = \log S(T)$ under the risk neutral measure P_Q and $k = \log K$ denotes the log-strike.

In order to ensure the existence of the Fourier transform, Carr and Madan (1999) modify the equation (59) by introducing the damping constant $\alpha > 0$ and consider the damped option price $c_T(k) = e^{\alpha k} C_T(k)$ and its Fourier transform $\varphi_{c_T}(t)$, i.e.

$$\begin{aligned} \varphi_{c_T}(t) &= \int_{-\infty}^{\infty} e^{itk} c_T(k) dk \\ c_T(k) &= \frac{1}{2\pi} \int_{-\infty}^{\infty} e^{-itk} \varphi_{c_T}(t) dt. \end{aligned} \quad (60)$$

Accordingly

$$\begin{aligned}
C_T(k) &= e^{-\alpha k} c_T(k) \\
&= e^{-\alpha k} \frac{1}{2\pi} \int_{-\infty}^{\infty} e^{-itk} \varphi_{c_T}(t) dt \\
&= e^{-\alpha k} \frac{1}{\pi} \int_0^{\infty} \operatorname{Re} [e^{-itk} \varphi_{c_T}(t)] dt
\end{aligned} \tag{61}$$

$\varphi_{c_T}(t)$ from the equation (61) is calculated in the appendix and can be written as

$$\varphi_{c_T}(t) = \frac{e^{-rT} \psi_T(t - (\alpha + 1)i)}{\alpha^2 + \alpha - t^2 + i(2\alpha + 1)t} \tag{62}$$

where $\psi_T(t)$ is characteristic function of the log-price process $S(T)$. This means that we can compute $C_T(k)$ by using the explicit Fourier transform of the damped option price in (62) (Hilpisch (2015)). We apply the right-hand rule to compute numerically the integral in the second equation in (61), more precisely, the integral

$$c_T(k) = \frac{e^{-\alpha k}}{\pi} \int_0^m \operatorname{Re} [e^{-itk} \varphi_{c_T}(t)] dt \tag{63}$$

where $m = Ndt$, dt is the discretization step, and N denotes the number of log-strikes used for calibration. The discretization reads

$$\hat{c}_T(k) \approx \operatorname{Re} \left[\frac{e^{-\alpha k}}{\pi} \sum_{j=1}^N e^{-iu_j k} \varphi_{c_T}(u_j) dt \right] \tag{64}$$

where $u_j = (j - 1)dt$. Cooley et al. (1969) introduce the numerical fast Fourier transform algorithm (FFT) which enables approximation of the integral of the above type by the discrete Fourier transform

$$w(u) = \sum_{j=1}^N e^{-i\frac{2\pi}{N}(j-1)(u-1)} x(j), \quad u = 1, \dots, N \tag{65}$$

for some vector $x(j)$ with $j = 1, \dots, N$.

Carr and Madan (1999) present the discretized integral in the trapezoid form from (64) as the discrete Fourier transform from (65). For every log-strike $k_v = -b + \eta(v - 1)$ with $v = 1, \dots, N$ we write

$$\begin{aligned}
\hat{c}_T(k_v) &\approx \operatorname{Re} \left[\frac{e^{-\alpha k_v}}{\pi} \sum_{j=1}^N e^{-i\eta dt(j-1)(v-1)} e^{ibu_j} \varphi_{c_T}(u_j) dt \right] \\
&= \operatorname{Re} \left[\frac{e^{-\alpha k_v}}{\pi} \sum_{j=1}^N e^{-i\frac{2\pi}{N}(j-1)(v-1)} e^{ibu_j} \varphi_{c_T}(u_j) dt \right]
\end{aligned} \tag{66}$$

where the relations $b = \frac{N\eta}{2}$ and $\eta dt = \frac{2\pi}{N}$ hold.

Instead of the top-right-rule, the Simpson rule can be applied to achieve higher accuracy for larger values of dt , which leads to

$$\hat{c}_T(k_v) = \operatorname{Re} \left[\frac{e^{-\alpha k_v}}{\pi} \sum_{j=1}^N e^{-i\frac{2\pi}{N}(j-1)(v-1)} e^{ibu_j} \varphi_{c_T}(u_j) \frac{dt}{3} (3 + (-1)^j - I\{j = 1\}) \right]. \tag{67}$$

The method is particularly useful in our case since all models under consideration constitute affine processes. Given the closed-form solution of the call price, we apply the Levenberg-Marquardt method with the objective

$$\inf_{\Theta_h} \sum_{i=1}^N w_i \left(C_i^{\Theta_h}(T_i, K_i) - C_i^{SV CJ}(T_i, K_i) \right)^2 \quad (68)$$

where $w_i = \frac{1}{n}$ and calibrate the parameters Θ_h of our hedge models against the simulated option prices for strikes K_i and maturities T_i . In our case we will have two sums since the number of strikes and maturities is not equal in (68) with the accuracy measure root mean square error

$$RMSE(\theta) = \frac{1}{\sqrt{N}} \sqrt{\inf_{\Theta_h} \sum_{i=1}^N w_i \left(C_i^{\Theta_h}(T_i, K_i) - C_i^{SV CJ}(T_i, K_i) \right)^2} \quad (69)$$

4 Simulation study

On behalf of the assumed calibrated parameters in table 1 and under the assumption that the dynamics of the asset price are described by the SDE in equation (9), $n = 1000000$ trajectories of the Euler discretized process denoted in equation (18) are simulated. We estimate unbiased estimators of European call options $C_{SVCJ}(T, K)$ with Monte Carlo Option Pricing described in section 2.4.2. On the basis of option prices generated for 11 strikes and 7 maturities, we calibrate the parameters of the hedge models introduced in section 3.2 according to the FFT-based procedure described in section 3.4. We then compute the sensitivities and the portfolio strategy ϕ for each hedge model and empirically perform Monte Carlo delta hedging. The self-financed hedging strategy explained in section 3.1 and is performed on every path and every time step. The resulting vector is the P & L distribution. We simulate 77 option prices with 7 strikes $K = \{70, 80, 90, 100, 110, 120, 130\}$ and 11 maturities $T = \{1\ m, 2\ m, 3\ m, 4\ m, 5\ m, 6\ m, 7\ m, 8\ m, 9\ m, 10\ m, 1\ y\}$. Table 2 illustrates all simulated ATM option prices with $K_{ATM} = 100$. The call prices for other strikes and maturities are presented in table 12 and table 13.

Call price	95 % Confidence Interval	Strike	Issuing Date	Maturity
9.35	[9.32, 9.39]	100	2019-07-04	2019-08-03
9.32	[9.29, 9.36]	100	2019-07-04	2019-09-02
9.29	[9.25, 9.32]	100	2019-07-04	2019-10-03
9.26	[9.22, 9.29]	100	2019-07-04	2019-11-02
9.23	[9.20, 9.26]	100	2019-07-04	2019-12-03
9.19	[9.16, 9.23]	100	2019-07-04	2020-01-02
9.16	[9.13, 9.19]	100	2019-07-04	2020-02-01
9.19	[9.10, 9.16]	100	2019-07-04	2020-03-03
9.10	[9.06, 9.13]	100	2019-07-04	2020-04-02
9.07	[9.03, 9.10]	100	2019-07-04	2020-05-03
9.03	[9.00, 9.06]	100	2019-07-04	2020-06-02

Table 2: Simulated ATM option prices for 11 maturities

 SVCJ_MC

4.1 Calibration of hedge models

Figure 4 illustrates the implied volatility surface for all 77 option prices $C_{SVCJ}(K, T)$ presented in table 2, table 12 and table 13. Moneyness is defined as $\frac{S(t)}{K}$.

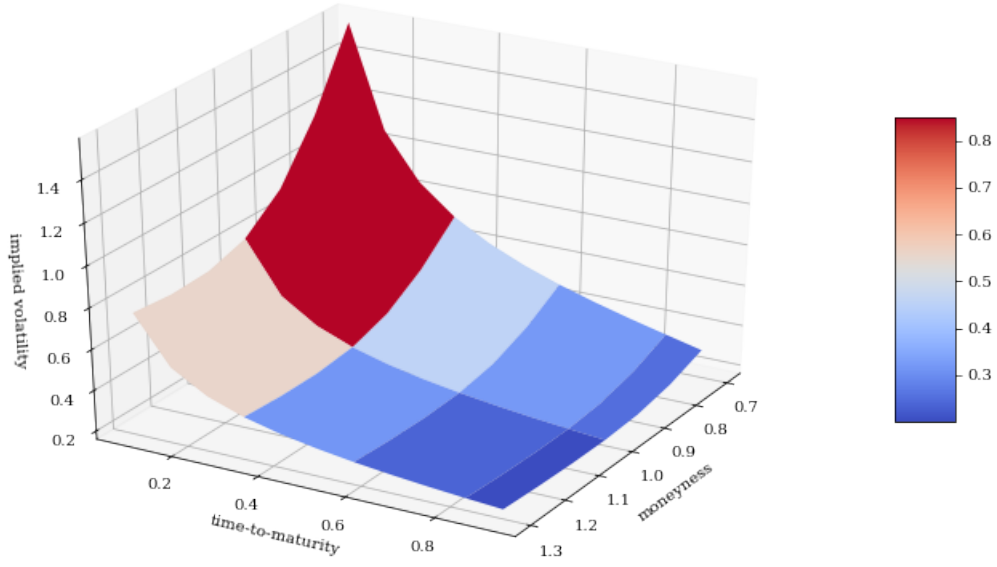



Figure 4: SVCJ implied volatility surface for 77 options

 SVCJ_MC

We calibrate the parameters of the hedge models with the FFT approach described in section 3.4. In the case of Black-Scholes, $\Theta = \{\sigma\}$ is the only parameter required for the calibration procedure in equation (68). We estimate σ across 77 option prices. The results of the calibration are presented in table 3. We report a $\sigma_{BS} = 0.287$ with a hedge error of 3.272.

Model	σ	MSE
Black-Scholes	0.287	3.272

Table 3: Calibrated parameter of the Black-Scholes model

 SVCJ_MC

The Heston (1993) model with the dynamics of the underlying described by equation (38) and the closed-form solution of the option price presented in equation (39) requires the estimation of 5 parameters $\Theta = \{V_0, \kappa_{heston}, \theta_{heston}, \sigma_{v_{heston}}, \rho_{heston}\}$. Table 4 presents the calibrated parameters of the Heston model.

Model	V_0	κ_{heston}	θ_{heston}	$\sigma_{v_{heston}}$	ρ_{heston}	MSE
Heston	3.406	67.521	0.006	0.920	-0.994	2.755

Table 4: Calibrated parameters of the Heston model

 SVCJ_MC

The calibration error in this model is fairly large. This indicates a bad fit. In section 3.2 we state that the Heston (1993) model is a special case of the generalized model with the dynamics under equation (9). We compare the calibrated parameters in table 4 to the parameters in table 1. In table 4, the calibrated parameter ρ_{heston} is negative. This is not in line with findings of Hou et al. (2019) summarized in section 2.5.1, where an inverse leverage effect is reported. The calibrated mean-reversion speed κ_{heston} , initial variance V_0 and σ_v are fairly high. On the contrary, in comparison to the mean-reversion level of the SVCJ in table 1, the calibrated mean-reversion level θ_{heston} is very small. Figure 5 presents the implied volatility surface of the Heston model.

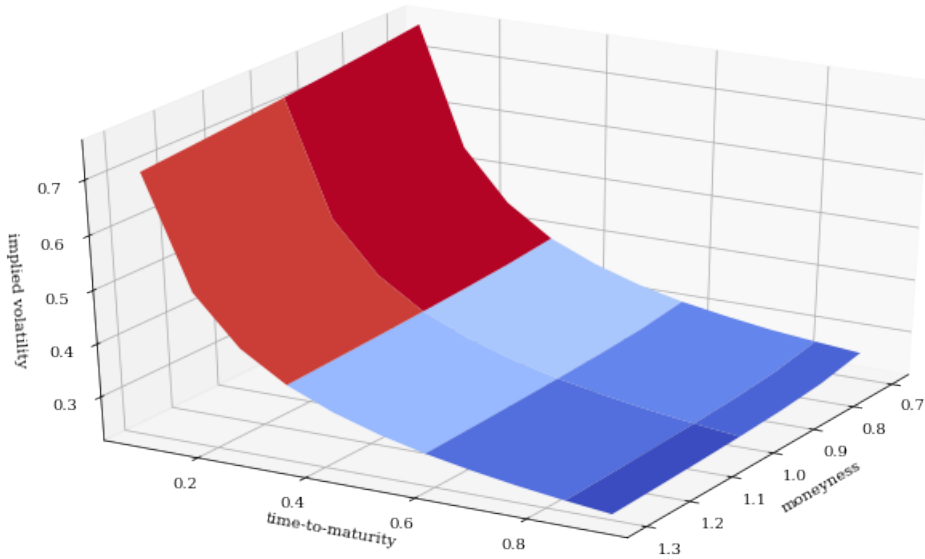


Figure 5: Implied volatility surface of the Heston model

 CRIXHEDGING

It is worth investigating in the shape of the implied volatility surface, because it is nearly flat across strikes. Therefore, we briefly summarize impact of certain parameters the shape of the implied

volatility surface. Bergomi (2015) states that κ_{heston} impacts the term-structure. As $\kappa_{heston} = 67.521$, we observe a very steep slope across maturities. Furthermore, σ_v impacts the convexity of the smile and $V(0)$ the ATM implied volatility. Lastly, ρ impacts the skew of the surface (Bergomi, 2015). Table 5 illustrates the calibrated parameters of the Merton Jump Diffusion Model.

Model	σ	λ_{merton}	$\mu_{j_{heston}}$	$\sigma_{j_{merton}}$	MSE
Merton	0.0000	5.191	-0.081	0.110	2.937

Table 5: Calibrated parameters of the Merton model

In table 5, λ is fairly high but σ is at 0. With respect to the asset dynamics described by equation (49), the asset price process under the risk-neutral measure P^* in equation (50) and the call price of an option given in equation (51), the calibrated parameters in table 5 indicate that this process is purely jump driven. There is no diffusion and the drift component is nearly zero. The volatility surface is illustrated in figure 6. The implied volatility surface has no particular shape. However, one can argue that the term-structure of the implied volatility surface is nearly flat and that there is evidence for a skew.

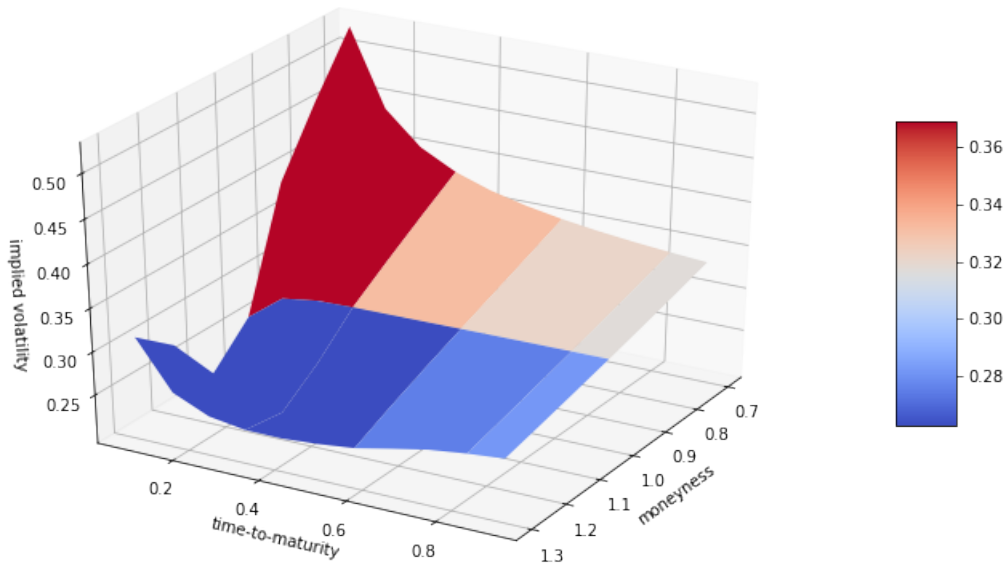


Figure 6: Implied volatility surface of the Merton model

5 Hedge performance of dynamic delta hedging

The purpose of this analysis is to show how the Δ of a hedge model reacts to various scenarios. This analysis relates to the interpretation in Marroni and Perdomo (2013). We observe how sensitivities react to moneyness and time to expiry. Further distinctions in special cases exceed the scope of this paper. For further information on this topic, the reader is recommended to look into Marroni and Perdomo (2013).

5.1 Black-Scholes

Figure 7a and figure 7b illustrate two simulated trajectories of the underlying asset $S(t)$. We assume the parameters from table 1 and consider an option with an ATM strike and a maturity of $\tau = 1$ year. The premium of this option can be read from table 2. The blue trajectory presents the Δ_{BS} of an option with an ATM strike, a maturity of $\tau = 1$ year and the calibrated parameter σ from table 3.

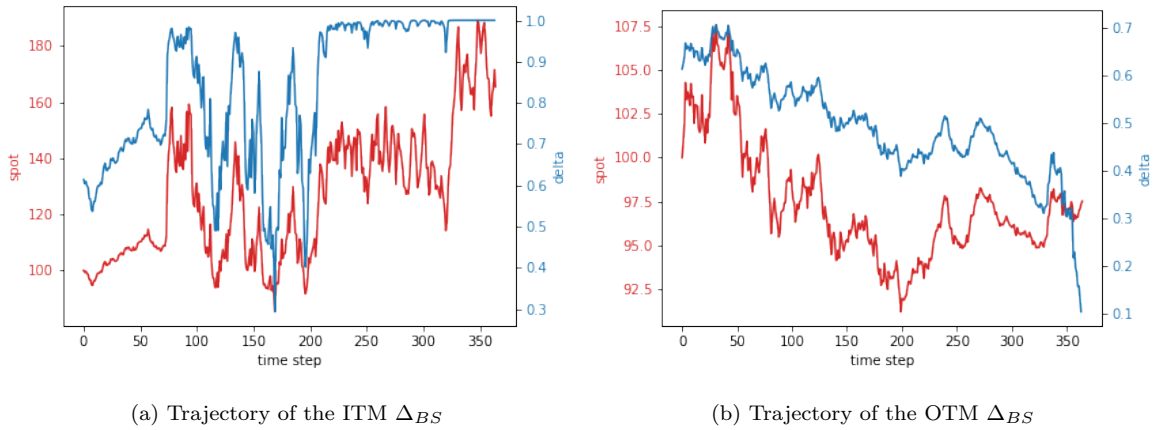


Figure 7: Trajectories of the misspecified delta Δ_{BS} in blue compared to the trajectory of the underlying $S(t)$ in red



The purpose of this illustration by cases is to show how Δ_{BS} reacts to discontinuities from jumps and stochastic volatility. The behavior of Δ_{BS} depends on various parameters. These include volatility, time-to-maturity and moneyness. At maturity, an option expires ITM or worthless. If the option expires ITM, $\Delta_{BS} = 1$. On the contrary, the option expires worthless and $\Delta_{BS} = 0$. Figure 7a illustrates a trajectory of the asset price process that incorporates large jump amplitudes and patterns of stochastic volatility. Throughout the entire period, the option written on the underlying $S(t)$ with the trajectory presented in figure 7a is ITM and this particular option expires deep ITM. In figure 7a,

we see that Δ_{BS} has the highest amplitudes ATM. This is not surprising, because ATM

$$\Delta_{BS}(S(t), t) = \frac{\partial C}{\partial S} = \Phi \left(\frac{\left(r - \frac{\sigma^2}{2}\right) \tau}{\sigma \sqrt{\tau}} + \sigma \sqrt{\tau} \right) \quad (70)$$

In the 4th quarter, the option is already deep ITM and Δ_{BS} is close to 1. We wish to focus on the period around day 350, where Δ_{BS} is already very close to 1. In this time frame we suddenly observe patterns of jumps and stochastic volatility in the trajectory of the asset price process $S(t)$. However, Δ_{BS} cannot react to those changes and expires at $\Delta_{BS} = 1$. Within this small time interval close to expiry, Δ_{BS} both over- and underestimates the market move. In the event of a large downward movement in the asset price, the option could expired worthless. We conclude that Δ_{BS} is unable to capture extreme events. In figure 7b, the trajectory of the underlying $S(t)$ has patterns of only few discontinuities. In this scenario, the option written on the underlying $S(t)$ is mostly OTM and expires worthless. In figure 7b, Δ_{BS} strongly reacts to market moves but does not readjust quickly enough to existent discontinuities in the price. Δ_{BS} cannot react quickly enough to jumps or stochastic volatility when the option is already deep OTM. In section 2.5.1, figure 3a illustrates various trajectories of the underlying $S(t)$ and we point on selected cases with large jumps or periods of extreme volatility. The misspecified hedge models is unable to capture these movements. We use figure 7a and figure 7b to illustrate how Δ_{BS} behaves when the option is ITM, ATM or OTM given some time-to-expiry. Overall, the examples in figure 7a and figure 7b illustrate that Δ_{BS} mostly captures the dynamics fairly well. In the scenario illustrated in 7b, due to a jump, the option nearly expires ATM. However, Δ_{BS} is unable to react to this change. Similarly, when the option is deep ITM such as in the scenario illustrated in figure 7a and close to maturity, Δ_{BS} remains very close to $\Delta_{BS} = 1$ and cannot react to large price drops. The conclusion is that Δ_{BS} fails to react to extreme cases. This is especially the case when the option is close-to-expiry. This is to some extent consistent with the results of Branger et al. (2012). The simple 'classic' BS slightly underperforms during regular periods and vastly underperforms during extreme movements (Branger et al., 2012).

In this hedge analysis we consider options with maturities of 3 months (3M), 6 months (6M), 9 months (9M) and 1 year (1Y). We choose 3 different strikes, namely K at-the-money (ATM) denoted by $K = K_{ATM}$ as well as $K_{0.95} = K_{ATM} \cdot 0.95$ and $K_{1.05} = K_{ATM} \cdot 1.05$. We observe the P & L relative to the option premium C_{SVCI} and evaluate the overall hedge performance based on the P & L distribution, the momentum quantiles and the hedge error. Table 6 illustrates the quantiles of the relative P & L from Δ_{BS} hedging an ATM option with different maturities. Selected moments of all relative P & Ls and the hedge error are presented in table 7. The hedging performance for $K_{0.95} = K_{ATM} \cdot 0.95$ and $K_{1.05} = K_{ATM} \cdot 1.05$ are in the appendix.

Quantile	3M	6M	9M	1Y
0.001	-5.753	-5.693	-5.335	-5.398
0.01	-2.203	-2.186	-2.147	-2.148
0.05	-0.467	-0.470	-0.406	-0.403
0.1	-0.283	-0.300	-0.259	-0.263
0.25	-0.101	-0.111	-0.100	-0.105
0.50	0.079	0.074	0.072	0.071
0.75	0.248	0.251	0.242	0.246
0.90	0.380	0.396	0.377	0.388
0.95	0.449	0.474	0.445	0.459
0.99	0.567	0.607	0.548	0.565
0.999	0.600	0.771	0.656	0.6569

Table 6: Quantiles of the Profit and Loss distribution where the hedge model is Black-Scholes for K_{ATM}



In table 6, the values of the relative P & L do not vary much across maturities. For illustration purposes, a representative relative P & L with $\tau = 9M$ and K_{ATM} is chosen to graphically illustrate the results from table 6. Figure 8 presents this graphical illustration. The quantiles of this P & L distribution can be read from column 3 of table 6. In figure 8, the losses are truncated to -300% . Some further P & L histograms for different strikes and maturities are presented in the appendix.

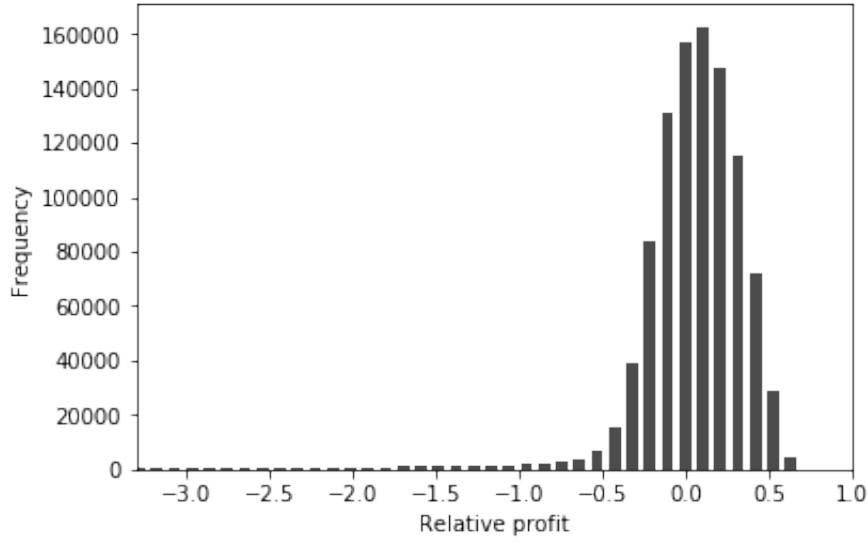


Figure 8: Relative PnL for 9M under misspecification with Black-Scholes for K_{ATM}

 CRIXHEDGING

	3M	6M	9M	1Y
standdev	0.520	0.521	0.488	0.500
skewness	-6.489	-6.558	-6.149	-7.917
kurtosis	79.021	106.098	92.449	149.697
hedge error	0.098	0.088	0.0825	0.0855

Table 7: Selected moments and the hedge error where the Hedge model is Black-Scholes for K_{ATM}

 CRIXHEDGING

In table 6, the median is close to zero across different maturities. Within the 5% to 99.9% quantile, relative gains and losses are of manageable size. It appears that the hedge performs well. The graphical illustration of the P & L distribution shows that the hedge fails in the left tail. In table 6, losses in the 1% quantile and especially in the 0.1% quantile are of severe magnitude. A comparison of table 6 to table 14 and table 16 shows that this observation is consistent across different strikes and maturities. The interpretation is that these losses result from extreme movements. Nevertheless, taking under consideration that the Black-Scholes model is the simplest model under consideration, the Δ_{BS} hedge performance is satisfactory.

5.2 Heston model

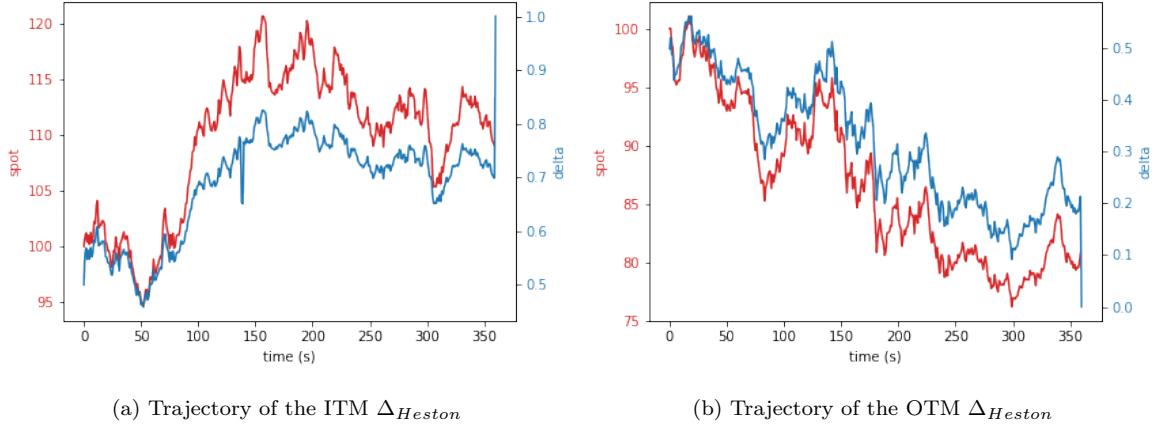


Figure 9: Trajectories of the misspecified delta Δ_{SV} in blue compared to the trajectory of the underlying $S(t)$ in red



Figure 9a and figure 9b illustrate two trajectories of the asset price process $S(t)$ and two trajectories of Δ_{SV} . The purpose is again to look at the behavior of the misspecified Δ_{SV} under consideration of moneyness (OTM, ATM and ITM) and time to maturity. As in section 5.1, a European call option with an ATM strike and a maturity of $\tau = 1$ year is written on the underlying $S(t)$. In figure 9a, the option is mainly ITM and expires ITM. According to this representative illustration, Δ_{SV} mainly accurately follows the movement of price. Shortly after $S(0)$ and in the forth quarter, the option is roughly ATM. Around this period, the trajectory of Δ_{SV} reveals that Δ_{SV} is very sensitive to the large jump and high volatility. ITM, changes in Δ_{SV} are small. ITM changes in Δ_{SV} to changes in the underlying are small. In other words, Γ_{SV} is small. In the second and fourth quarter, it appears that Δ_{SV} overestimated the movement. Close to expiry and deep ITM, changes in Δ_{SV} are larger than changes Δ_{BS} . We interpret from figure 3a in in section 2.5.1 that the main driver is stochastic volatility. In figure 9b, the option written on the underlying is deep OTM. In this case, volatility and jumps are favored (Marroni and Perdomo, 2013). The trajectory of the underlying has some discontinuities from jumps and patterns of stochastic volatility. It appears that Δ_{SV} again captures the movements in accurate manner. In total, the Δ_{SV} from the Heston (1993) appears to fit the market move well, yet tends to overestimate moments of high volatility. Table 8 illustrates the quantiles of the relative Profit and Loss distribution from delta hedging a call option written on the underlying $S(t)$ for various maturities and the K_{ATM} strike and table 9 presents selected moments of all relative P & Ls and the hedge error. Again, the hedge performance appears not very different across different maturities. The 50%-quantile is again close to zero. In comparison to table 6, the interquantile in table 8 is wider across all maturities.

Quantile	3M	6M	9M	1Y
0.001	-8.547	-6.845	-7.369	-7.83
0.01	-2.699	-2.266	-2.398	-2.647
0.05	-0.641	-0.610	-0.557	-0.589
0.10	-0.424	-0.412	-0.343	-0.372
0.25	-0.164	-0.172	-0.109	-0.131
0.50	0.097	0.080	0.137	0.0803
0.75	0.332	0.325	0.377	0.356
0.90	0.493	0.486	0.531	0.518
0.95	0.573	0.563	0.598	0.589
0.99	0.724	0.692	0.72	0.708
0.999	3.946	5.982	7.737	5.138

Table 8: Quantiles of the Profit and Loss distribution where the Hedge model is Heston ATM

	3M	6M	9M	1Y
standdev	1.016	0.779	0.78	0.998
skewness	-10.9	-2.806	6.095	-13.911
kurtosis	414.028	119.162	307.944	63.98
hedge error	0.168	0.131	0.132	0.164

Table 9: Selected moments and the hedge error where the Hedge model is Heston for K_{ATM}

Figure 10 illustrates the representative P & L from Δ_{heston} -hedging for K_{ATM} and $\tau = 9$ M. Losses were truncated in the same manner as in section 5.1.

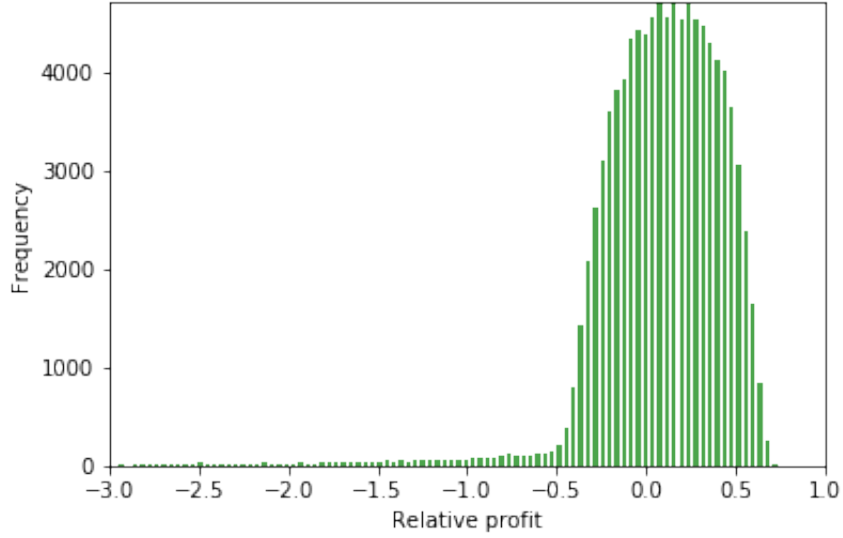


Figure 10: Relative PnL for 9M under misspecification with Heston for K_{ATM}

 CRIXHEDGING

The hedge performance in the 5% quantile up to the 95 % quantile is satisfactory. The 1% and 0.1% quantile illustrate that the hedge performs poorly in the left tail. The hedge portfolio clearly underestimates risk more severely than the simple Black-Scholes model. These losses could result from large jumps. In the right tail, risk is overestimated. In figure 9a, we have seen that Δ_{SV} captures the movement of the asset price process fairly well. On the downside, it may overreact to movements. In conclusion, the hedge performance of the Heston (1993) model is satisfactory. We believe that large losses result from extreme movements. This is also in line with the results from Branger et al. (2012).

5.3 Merton jump diffusion

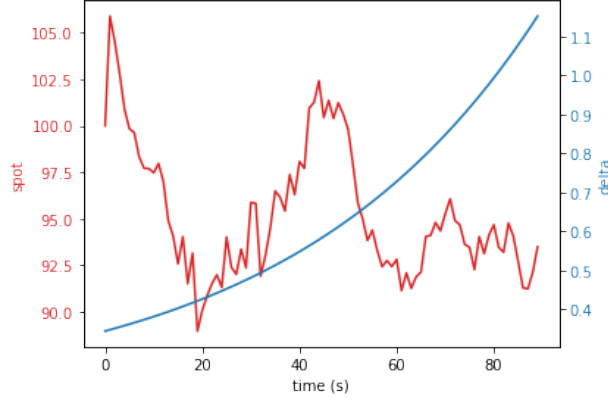


Figure 11: Trajectories of the misspecified delta Δ_{Merton} in blue compared to the trajectory of the underlying $S(t)$ in red



Lastly, we observe the hedge performance of the Merton (1976) jump diffusion model. Figure 11 illustrates one trajectory of the Δ_{Merton} compared to the trajectory of the asset price process $S(t)$. According to the calibration results in table 5 the volatility parameter $\sigma = 0$. From equation (52), Δ_{Merton} depends on σ , κ and r_i and is expressed by an infinite series. This means that Δ_{Merton} only depends on the deterministic drift component and a jump component. The movement of the Δ_{Merton} is entirely deterministic and unable to capture any discontinuities from jumps or stochastic volatility. Table 10 presents the quantiles of the relative P & L from Δ_{Merton} -hedging. As the hedge performance of this model is also invariant across tenors, we select a graphical representative of the relative P % L for $\tau = 9$ M that is illustrated in figure 12. In the interquantile range, gains and losses appear of tolerable size. In the left tail, losses are of large magnitude. In the 1 % quantile, the losses are as severe as in the Heston model. In comparison to table 8 and table 6, this hedge already fails in the 5 % quantile and severe losses are already observed in the 10 % quantile. There is clear evidence for tail risk. On the gain side, the observed relative profit is much larger than from Δ_{BS} - and Δ_{Heston} - hedging. In the right tail gains are already very large at the 90 % quantile. This hedge misspecification provides the worst performing hedge performances among the 3 models. For a higher strike, losses are even larger. Table 21 illustrates the quantiles from hedging the short position in the option with a strike of $K = K_{ATM} \cdot 1.05$. The median is already at the loss side. In the 0.1% and 1% quantile, losses are extreme. In the right tail, gains are very large. This hedge model clearly underperforms. Branger et al. (2012) report that the Merton (1976) model performs well in extreme cases but fails to hedge under regular circumstances. We illustrated that the main driver of this process is stochastic volatility, but jumps can lead large amplitudes and therefore large losses. The

jump component of the Merton model with the dynamics described in equation (49) is a simple compound Poisson process with lognormally distributed jumps. This model is misspecified in terms of volatility and jump sizes. This is compensated in the calibration in the following manner. The jump intensity of λ is very large. However, this process includes no volatility at all. Therefore, the fit is very poor.

Quantile	3M	6M	9M	1Y
0.001	-6.699	-6.539	-6.519	-6.761
0.01	-3.085	-2.999	-3.034	-3.001
0.05	-1.305	-1.314	-1.310	-1.328
0.10	-0.883	-0.888	-0.873	-0.885
0.25	-0.347	-0.351	-0.326	-0.323
0.50	0.130	0.132	0.153	0.156
0.75	0.529	0.531	0.535	0.539
0.90	0.843	0.837	0.832	0.832
0.95	1.022	1.014	1.007	1.002
0.990	1.361	1.357	1.351	1.347
0.999	2.203	2.066	1.961	1.990

Table 10: Quantiles of the Profit and Loss distribution where the Hedge model is Merton ATM

	3M	6M	9M	1Y
standdev	0.66	0.657	0.652	0.662
skewness	-3.796	-3.943	-4.014	-5.905
kurtosis	51.288	51.205	69.592	235.123
hedge error 0.0840	0.0843	0.083	0.0843	0.0847

Table 11: Selected moments and the hedge error where the Hedge model is Merton for K_{ATM}

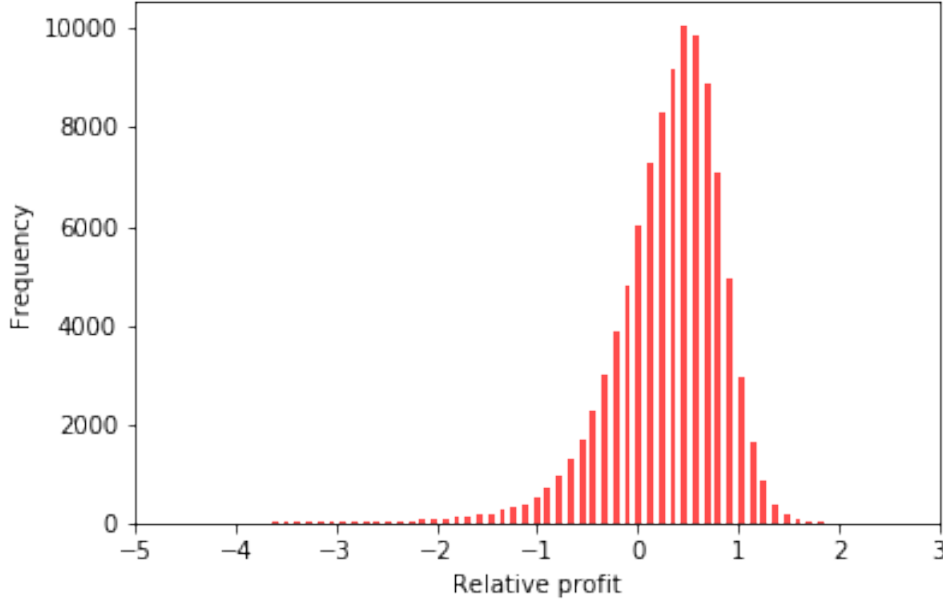


Figure 12: Relative PnL for $\tau = 9M$ under misspecification with Merton for K_{ATM}

5.4 Comparison of Δ -hedges

We compare the hedge performance of our models. All 3 models fail in the left tail. In the 0.1%-quantile, losses are extreme. We have illustrated in figure 2 and figure 3a how large amplitudes of jumps in returns can become. Therefore, the interpretation is that losses in 0.1 % and the 1 % quantile result from extreme jumps. In the 5 % quantile, there is a drastic difference in terms of hedge performance. The losses in the Merton model are of extreme magnitude. Losses up to the 10 % quantile are much large than in the other models. In total, the Merton (1976) model fails to hedge risk in the first quantile. The Heston and the Black-Scholes model perform significantly better. Among the two, the Black-Scholes model outperforms the Heston model. In the lower 50 % of the observations, the Black-Scholes model performs slightly better. Around the median, the performance is roughly comparable. On the gain side, the Heston model and the Merton model outperform the Black-Scholes model. The Merton model already reports very high gains in the 90 % and 95 % quantile. Extreme gains are the largest in the case of the Heston model. We believe that this is due to the movement of Δ . When Δ_{BS} is for example deep ITM and close to maturity, changes in Δ_{BS} are fairly small and it cannot react to large discontinuities in short time intervals. The Δ_{SV} is more flexible. Due to bad calibration, Δ_{Merton} does not react any changes and therefore either outperforms or underperforms.

6 Conclusion

We investigate hedging a model with a data-generating process $S(t)$ that tries to mimic the behavior of assets on cryptocurrency markets. Simulated option prices are extremely high. We observe the dynamics of the asset price process $S(t)$ and suspect that the main driver of the movements is stochastic volatility. According to our simulation study, hedging under misspecification can lead to a decent hedge performance during regular market moves. However, we find that a strategy cannot correspond quickly enough to abrupt changes from large jumps or volatile periods when approaching maturity. Our hedge simulation illustrates extreme losses in the left tail of the relative P & L in all hedging models. Our interpretation is that those losses result from single extreme events where jumps are of very high amplitude. The hedge performance of the Heston (1993) model is sophisticated, yet it can lead to extremes in both directions. The strategy can adjust to changes even close to maturity, but it could overestimate the effect of minor jumps and cannot react to extreme movements. The Black-Scholes model has a decent hedge performance. However, losses in the left tail are again extreme and close to maturity and deep ITM or OTM, Δ_{BS} is unable to react to discontinuities or larger movements. The worst-performing model is the Merton model. As a result from poor calibration, the Merton cannot react to the movement of the underlying and therefore over- and underestimates risk. The recommendation is that this simple model should be avoided.

In conclusion, from a market maker's perspective, pricing and hedging in a market with such dynamics is costly and often very risky. This study aims to motivate further investigations on risk management aspects in cryptocurrency markets.

A Appendix

A.1 Derivation of the Fourier transform of the damped call price

The call price can be rewritten as

$$\begin{aligned}
C_T(k) &= e^{-\alpha k} c_T(k) \\
&= e^{-\alpha k} \frac{1}{2\pi} \int_{-\infty}^{\infty} e^{-itk} \varphi_{c_T}(t) dt \\
&= e^{-\alpha k} \frac{1}{\pi} \int_0^{\infty} e^{-itk} \varphi_{c_T}(t) dt
\end{aligned} \tag{71}$$

The last equality holds because φ_{c_T} is odd in the imaginary part and even in the real part. For the Fourier transform of the damped call price we write

$$\begin{aligned}
\varphi_{c_T}(t) &= \int_{-\infty}^{\infty} e^{itk} c_T(k) dk \\
&= e^{-rT} \int_{-\infty}^{\infty} e^{itk} \left(\int_k^{\infty} e^{\alpha k} (e^s - e^k) q_T(s) ds \right) dk \\
&= e^{-rT} \int_{-\infty}^{\infty} q_T(s) \left(\int_{-\infty}^s e^{itk} e^{\alpha k} (e^s - e^k) dk \right) ds
\end{aligned} \tag{72}$$

The integral inside can be written

$$\begin{aligned}
\int_{-\infty}^s e^{itk} e^{\alpha k} (e^s - e^k) dk &= e^s \int_{-\infty}^s e^{(it+\alpha)k} dk - \int_{-\infty}^s e^{(it+1+\alpha)k} dk \\
&= \frac{e^s}{it+\alpha} \left[e^{(it+\alpha)k} \right]_{-\infty}^s - \frac{1}{it+1+\alpha} \left[e^{(it+1+\alpha)k} \right]_{-\infty}^s \\
&= \frac{e^{(it+1+\alpha)s}}{it+\alpha} - \frac{e^{(it+1+\alpha)s}}{it+1+\alpha} \\
&= \frac{e^{(it+1+\alpha)s}}{(it+\alpha)(it+1+\alpha)}
\end{aligned} \tag{73}$$

Finally we get for the Fourier transform of the damped call price

$$\varphi_{c_T}(t) = \frac{e^{-rT} \varphi_{c_T}(t - (\alpha + 1)i)}{\alpha^2 + \alpha - t^2 + i(2\alpha + 1)t} \tag{74}$$

A.2 Tables

Call price	95 % Confidence Interval	Strike	Issuing Date	Maturity
4.91	[4.88, 4.95]	110.0	2019-07-04	2019-11-02
4.90	[4.87, 4.93]	110.0	2019-07-04	2019-12-03
4.88	[4.85, 4.91]	110.0	2019-07-04	2020-01-02
4.86	[4.84, 4.89]	110.0	2019-07-04	2020-02-01
4.85	[4.82, 4.87]	110.0	2019-07-04	2020-03-03
4.83	[4.80, 4.86]	110.0	2019-07-04	2020-04-02
4.81	[4.78, 4.84]	110.0	2019-07-04	2020-05-03
4.80	[4.78, 4.82]	110.0	2019-07-04	2020-06-02
2.60	[2.56, 2.62]	120.0	2019-07-04	2019-08-03
2.58	[2.55, 2.60]	120.0	2019-07-04	2019-09-02
2.57	[2.54, 2.69]	120.0	2019-07-04	2019-10-03
2.56	[2.54, 2.59]	120.0	2019-07-04	2019-11-02
2.55	[2.53, 2.58]	120.0	2019-07-04	2019-12-03
2.54	[2.52, 2.57]	120.0	2019-07-04	2020-01-02
2.54	[2.51, 2.56]	120.0	2019-07-04	2020-02-01
2.53	[2.50, 2.55]	120.0	2019-07-04	2020-03-03
2.52	[2.49, 2.543]	120.0	2019-07-04	2020-04-02
2.51	[2.48, 2.53]	120.0	2019-07-04	2020-05-03
2.50	[2.47, 2.52]	120.0	2019-07-04	2020-06-02
1.41	[1.39, 1.43]	130.0	2019-07-04	2019-08-03
1.41	[1.39, 1.43]	130.0	2019-07-04	2019-09-02
1.40	[1.38, 1.42]	130.0	2019-07-04	2019-10-03
1.40	[1.38, 1.42]	130.0	2019-07-04	2019-11-02
1.40	[1.37, 1.42]	130.0	2019-07-04	2019-12-03
1.39	[1.37, 1.41]	130.0	2019-07-04	2020-01-02
1.39	[1.36, 1.41]	130.0	2019-07-04	2020-02-01
1.38	[1.36, 1.40]	130.0	2019-07-04	2020-03-03
1.38	[1.35, 1.40]	130.0	2019-07-04	2020-04-02
1.37	[1.35, 1.34]	130.0	2019-07-04	2020-05-03
1.37	[1.34, 1.38]	130.0	2019-07-04	2020-06-02

Table 12: Option pricing with Monte Carlo option pricing for 7 strikes and 11 maturities

Call price	95 % Confidence Interval	Strike	Issuing Date	Maturity
34.68	[34.64, 34.72]	70.0	2019-07-04	2019-08-03
34.560	[34.51, 34.60]	70.0	2019-07-04	2019-09-02
34.44	[34.39, 34.48]	70.0	2019-07-04	2019-10-03
34.32	[34.27, 34.36]	70.0	2019-07-04	2019-11-02
34.20	[34.16, 34.24]	70.0	2019-07-04	2019-12-03
34.08	[34.04, 34.12]	70.0	2019-07-04	2020-01-02
33.96	[33.92, 34.00]	70.0	2019-07-04	2020-02-01
33.84	[33.80, 33.88]	70.0	2019-07-04	2020-03-03
33.72	[33.68, 33.76]	70.0	2019-07-04	2020-04-02
33.61	[33.57, 33.64]	70.0	2019-07-04	2020-05-03
33.49	[33.45, 33.53]	70.0	2019-07-04	2020-06-02
25.03	[24.99, 25.07]	80.0	2019-07-04	2019-08-03
24.94	[24.91, 24.98]	80.0	2019-07-04	2019-09-02
24.86	[24.82, 24.90]	80.0	2019-07-04	2019-10-03
24.78	[24.74, 24.82]	80.0	2019-07-04	2019-11-02
24.69	[24.65, 24.73]	80.0	2019-07-04	2019-12-03
24.60	[24.56, 24.64]	80.0	2019-07-04	2020-01-02
24.52	[24.48, 24.56]	80.0	2019-07-04	2020-02-01
24.43	[24.39, 24.47]	80.0	2019-07-04	2020-03-03
24.35	[24.30, 24.39]	80.0	2019-07-04	2020-04-02
24.26	[24.22, 24.30]	80.0	2019-07-04	2020-05-03
24.18	[24.13, 24.21]	80.0	2019-07-04	2020-06-02
16.27	[16.19, 16.26]	90.0	2019-07-04	2019-08-03
16.17	[16.13, 16.20]	90.0	2019-07-04	2019-09-02
16.11	[16.08, 16.15]	90.0	2019-07-04	2019-10-03
16.06	[16.02, 16.10]	90.0	2019-07-04	2019-11-02
16.00	[15.96, 16.04]	90.0	2019-07-04	2019-12-03
15.94	[15.91, 15.98]	90.0	2019-07-04	2020-01-02
15.88	[15.85, 15.93]	90.0	2019-07-04	2020-02-01
15.83	[15.80, 15.87]	90.0	2019-07-04	2020-03-03

Table 13: Option pricing with Monte Carlo option pricing for 7 strikes and 11 maturities

Quantile	3m	6m	9m	1y
0.001	-4.069	-3.856	-3.728	-3.553
0.01	-1.430	-1.394	-1.306	-1.349
0.05	-0.099	-0.096	-0.090	-0.107
0.10	0.001	0.006	0.016	0.001
0.25	0.151	0.161	0.176	0.171
0.50	0.320	0.321	0.332	0.328
0.75	0.467	0.459	0.465	0.463
0.90	0.574	0.561	0.566	0.565
0.95	0.632	0.612	0.617	0.618
0.99	0.737	0.696	0.697	0.695
0.999	1.216	0.914	0.833	0.781

Table 14: Quantiles of the relative P &L distribution where the Hedge model is Black-Scholes for $K_{0.95}$

	3m	6m	9m	1y
standdev	0.403	0.397	0.376	0.382
skewness	-5.595	-5.278	-5.238	-6.901
kurtosis	64.799	89.284	75.351	119.393
hedge error	0.0512	0.0509	0.0477	0.049

Table 15: Selected moments and the hedge error where the Hedge model is Black-Scholes for $K_{0.95}$

Quantile	3m	6m	9m	1y
0.001	-8.392	-8.334	-8.008	-8.101
0.01	-3.429	-3.335	-3.285	-3.347
0.05	-1.263	-1.224	-1.173	-1.214
0.10	-0.994	-0.985	-0.953	-0.986
0.25	-0.594	-0.624	-0.599	-0.625
0.50	-0.222	-0.241	-0.220	-0.240
0.75	0.040	0.029	0.049	0.040
0.90	0.226	0.221	0.246	0.244
0.95	0.312	0.312	0.339	0.345
0.99	0.447	0.450	0.477	0.488
0.999	12.549	21.728	21.600	0.600

Table 16: Quantiles of the relative P &L distribution where the Hedge model is Black-Scholes for $K_{1.05}$

	3m	6m	9m	1y
std	0.769	0.764	0.735	0.757
skew	-5.667	-5.291	-5.226	-6.535
kurtosis	64.569	79.03	70.292	113.664
hedge error	0.1778	0.178	0.170	0.176

Table 17: Selected moments and the hedge error where the Hedge model is Black-Scholes for $K_{1.05}$

Quantile	3m	6m	9m	1y
0.001	-4.771	-4.801	-4.636	-4.801
0.010	-2.057	-1.986	-2.019	-1.986
0.050	-0.720	-0.733	-0.724	-0.733
0.100	-0.403	-0.401	-0.396	-0.401
0.250	-0.001	0.020	0.015	0.020
0.500	0.358	0.379	0.374	0.379
0.750	0.657	0.665	0.662	0.665
0.900	0.893	0.885	0.885	0.885
0.950	1.027	1.013	1.016	1.013
0.990	1.281	1.271	1.275	1.271
0.999	1.914	1.752	1.732	1.752

Table 18: Quantiles of the relative Profit and Loss distribution where the Hedge model is Merton for $K_{0.95}$

	3m	6m	9m	1y
standdev	0.660	0.662	0.652	0.657
skewness	-3.796	-5.905	-4.014	-3.943
kurtosis	51.288	235.123	69.592	51.205
hedge error	0.084	0.085	0.083	0.0843

Table 19: Selected moments and the hedge error where the Hedge model is Merton for $K_{0.95}$

Quantile	3m	6m	9m	1y
0.001	-9.511	-9.313	-9.247	-9.605
0.010	-4.584	-4.477	-4.504	-4.476
0.050	-2.158	-2.176	-2.159	-2.192
0.100	-1.582	-1.594	-1.564	-1.588
0.250	-0.852	-0.860	-0.820	-0.821
0.500	-0.201	-0.202	-0.168	-0.167
0.750	0.343	0.344	0.352	0.355
0.900	0.771	0.762	0.756	0.756
0.950	1.014	1.003	0.994	0.988
0.990	1.476	1.472	1.463	1.458
0.999	2.624	2.440	2.292	2.335

Table 20: Quantiles of the relative Profit and Loss distribution where the Hedge model is Merton for $K_{1.05}$

	3m	6m	9m	1y
standdev	1.198	1.206	1.181	1.197
skewness	-3.796	-5.905	-4.014	-3.943
kurtosis	51.288	235.123	69.592	51.205
hedge error	0.277	0.276	0.272	0.290

Table 21: Selected moments and the hedge error where the Hedge model is Merton for $K_{1.05}$

Quantile	3m	6m	9m	1y
0.001	-4.069	-3.856	-3.728	-3.553
0.01	-1.430	-1.394	-1.306	-1.349
0.05	-0.099	-0.096	-0.090	-0.107
0.10	0.001	0.006	0.016	0.001
0.25	0.151	0.161	0.176	0.171
0.50	0.320	0.321	0.332	0.328
0.75	0.467	0.459	0.465	0.463
0.90	0.574	0.561	0.566	0.565
0.95	0.632	0.612	0.617	0.618
0.99	0.737	0.696	0.697	0.695
0.999	1.216	0.914	0.833	0.781

Table 22: Quantiles of the relative Profit and Loss distribution where the Hedge model is Heston for $K_{0.95}$

Quantile	3m	6m	9m	1y
0.001	-6.072	-4.887	-5.350	-10.823
0.01	-1.679	-1.472	-1.577	-4.042
0.05	-0.184	-0.151	-0.120	-1.441
0.1	-0.064	-0.04	-0.004	-1.107
0.25	0.121	0.134	0.171	-0.554
0.50	0.32	0.323	0.355	-0.554
0.75	0.508	0.500	0.527	0.160
0.90	0.644	0.623	0.650	0.374
0.95	0.614	0.714	0.701	0.473
0.99	0.875	0.819	0.834	0.646
0.999	3.540	4.819	5.275	6.527

Table 23: Quantiles of the relative Profit and Loss distribution where the Hedge model is Heston for $K_{1.05}$

References

- ALBRECHER, H., A. BINDER, V. LAUTSCHAM, AND P. MAYER (2013): *Introduction to Quantitative Methods for Financial Markets*, Springer.
- BAKSHI, G., C. CAO, AND Z. CHEN (1997): “Empirical Performance of Alternative Option Pricing Models,” *Journal of Finance*, 52, 2003–49.
- BANDI, F. AND R. RENO (2016): “Price and volatility co-jumps,” *Journal of Financial Economics*, 119, 107–146.
- BATES, D. S. (1996): “Jumps and stochastic volatility: Exchange rate processes implicit in Deutsche mark options,” *The Review of Financial Studies*, 9, 69–107.
- BELAYGOROD, A. AND J. M. OLIN (2005): “Solving Continuous Time Affine Jump-Diffusion Models for Econometric Inference,” *Working paper*.
- BERGOMI, L. (2015): *Stochastic Volatility Modeling*, Chapman and Hall/CRC Financial Mathematics Series, CRC Press.
- BLACK, F. AND M. SCHOLES (1973): “The Pricing of Options and Corporate Liabilities,” *Journal of Political Economy*, 81, 637–54.
- BORAK, S., K. DETLEFSEN, AND W. K. HÄRDLE (2005): “FFT Based Option Pricing,” .
- BOYLE, P. P. (1977): “Options: A Monte Carlo approach,” *Journal of Financial Economics*, 4, 323–338.
- BRANGER, N., A. HANSIS, AND C. SCHLAG (2010): “Expected Option Returns and the Structure of Jump Risk Premia,” *Working paper*.
- BRANGER, N., C. SCHLAG, E. SCHNEIDER, AND N. SEEGER (2012): “Hedging under model misspecification: all risk factors are equal, but some are more equal than others...” *The journal of futures markets*, Vol.32, No. 5, 397-430 (2012).
- BROADIE, M., M. CHERNOV, AND M. JOHANNES (2007): “Model specification and risk premia: Evidence from futures options,” *The Journal of Finance*, 62, 1453–1490.
- BROADIE, M. AND . KAYA (2006): “Exact Simulation of Stochastic Volatility and Other Affine Jump Diffusion Processes,” *Operations Research*, 54, 217–231.
- CARR, P. AND D. B. MADAN (1999): “Option Valuation Using the Fast Fourier Transform,” *Journal of Computational Finance*, 2, 61–73.
- CHEN, S., C. Y.-H. CHEN, W. K. HÄRDLE, T. M. LEE, AND B. ONG (2018): “Econometric Analysis of a Cryptocurrency Index for Portfolio Investment,” in *Handbook of Blockchain, Digital Finance, and Inclusion*, vol. 1, chap. 8, 175–206.

- CHERNOV, M., A. GALLANT, E. GHYSELS, AND G. TAUCHEN (2003): “Alternative models for stock price dynamics,” *Journal of Econometrics*, 116, 225–257.
- CIZEK, P., W. K. HÄRDLE, AND R. WERON (2011): *Statistical Tools for Finance and Insurance*, Springer, 2nd ed.
- CONT, R. AND P. TANKOV (2003): *Financial Modelling With Jump Processes*, vol. 1st edition, Chapman & Hall/CRC Financial Mathematics Series.
- COOLEY, J. W., P. A. W. LEWIS, AND P. D. WELCH (1969): “The Fast Fourier Transform and Its Applications,” *IEEE Trans. on Educ.*, 12, 27–34.
- DETERING, N. AND N. PACKHAM (2015): “Model risk in incomplete markets with jumps,” in *Innovations in Risk Management*, ed. by K. Glau, M. Scherer, and R. Zagst, vol. 99 of *Springer Proceedings in Mathematics & Statistics*, 39–56.
- DUFFIE, D., J. PAN, AND K. SINGLETON (2000): “Transform analysis and asset pricing for affine jump diffusions,” *Econometrica*, 68, 1343–1376.
- EL KAROUI, N., M. JEANBLANC-PICQUÉ, AND S. E. SHREVE (1998): “Robustness of the Black and Scholes Formula,” .
- ERAKER, B. (2004): “Do stock prices and volatility jump? Reconciling evidence from spot and option prices,” *The Journal of Finance*, 59, 1367–1403.
- ERAKER, B., M. JOHANNES, AND N. POLSON (2003): “The impact of jumps in volatility and returns,” *The Journal of Finance*, 58, 1269–1300.
- FÖLLMER, H. AND D. SONDERMANN (1986): “Hedging of nonredundant contingent claims,” 21.
- FRANKE, J., W. K. HÄRDLE, AND C. M. HAFNER (2015): *Statistics of Financial Markets*, 4th ed., Springer Verlag Heidelberg.
- GIRSANOV, I. V. (1960): “On transforming a certain class of stochastic processes by absolutely continuous substitution of measures,” *Theory of Probability & Its Applications*, 5, 285–301.
- GLASSERMAN, P. (2004): *Monte Carlo methods in financial engineering*, New York: Springer.
- GREEN, T. C. AND S. FIGLEWSKI (1999): “Market Risk and Model Risk for a Financial Institution Writing Options,” *Journal of Finance*, 54, 1465–1499.
- HÄRDLE, W. K. AND C. H. REULE, RAPHAEL (2019): “Understanding Cryptocurrencies,” *Journal of Financial Economics*, forthcoming.
- HESTON, S. L. (1993): “A closed-form solution for options with stochastic volatility with applications to bond and currency options,” *The review of financial studies*, 6, 327–343.

- HILPISCH, Y. (2014): *Python for Finance: Analyze Big Financial Data*, O'Reilly Media, Inc., 1st ed.
- (2015): *Derivatives Analytics with Python: Data Analysis, Models, Simulation, Calibration and Hedging*, O'Reilly Media, Inc., 1st ed.
- HOU, A., W. WANG, K. CHEN, AND W. K. CYH, HÄRDLE (2019): “Pricing cryptocurrency options: the case of CRIX and Bitcoin,” *Journal of Financial Econometrics*, *forthcoming*.
- HULL, J. (2006): *Options, futures, and other derivatives*, Upper Saddle River, NJ [u.a.]: Pearson Prentice Hall, 6. ed., pearson internat. ed ed.
- JEANBLANC, MONIQUE, Y. M. C. M. (2009): *Mathematical Methods for Financial Markets*, Springer Finance Textbooks.
- JOHANNES, M. AND N. POLSON (2009): “MCMC methods for continuous-time financial econometrics,” *Handbook of Financial Econometrics*, 2.
- KIENITZ, J. AND D. WETTERAU (2013): “Financial Modelling: Theory, Implementation and Practice with MATLAB Source,” .
- KURPIEL, A. AND T. RONCALLI (1999): “Option Hedging with Stochastic Volatility,” .
- MAKAROV, I. AND A. SCHOAR (2019): “Trading and arbitrage in cryptocurrency markets,” *Journal of Financial Economics*, In press.
- MARRONI, L. AND I. PERDOMO (2013): *Pricing and Hedging Financial Derivatives: A Guide for Practitioners*, vol. 1st edition, The Wiley Finance Series.
- MERTON, R. C. (1976): “Option pricing when underlying stock returns are discontinuous,” *Journal of financial economics*, 3, 125–144.
- NAKAMOTO, S. (2008): “Bitcoin: A peer-to-peer electronic cash system,” .
- PAN, J. (2002): “The Jump-Risk Premia Implicit in Options: Evidence From an Integrated Time-Series Study,” *Journal of Financial Economics*, 63, 3–50.
- PEREZ, I. (2018): “Graphical User Interface for pricing Cryptocurrency Options under the Stochastic Volatility with Correlated Jumps model,” *Humboldt-University Berlin*.
- POKLEWSKI-KOZIELL, W. (2012): “STOCHASTIC VOLATILITY MODELS: CALIBRATION, PRICING AND HEDGING,” *University of the Witwatersrand*.
- POULSEN, R., K. SCHENK-HOPP, AND C.-O. EWALD (2009): “Risk minimization in stochastic volatility models: model risk and empirical performance,” *Quantitative Finance*, 9, 693–704.
- SCAILLET, O., A. TRECCANI, AND C. TREVISAN (2018): “High-frequency jump analysis of the bitcoin market,” *Journal of Financial Econometrics*, *in print*.

- SCHWARTZ, E. AND A. TROLLED (2009): “Unspanned stochastic volatility and the pricing of commodity derivatives,” *Review of financial studies*, 22, 4423-4461.
- SHREVE, S. E. (2004): *Stochastic calculus for finance 2, Continuous-time models*, New York, NY; Heidelberg: Springer.
- SUN, Y., G. YUAN, S. GUO, J. LIU, AND S. YUAN (2015): “Does model misspecification matter for hedging? computational finance experiment based approach,” *International Journal of Financial Engineering (IJFE)*, 02, 1–21.
- TRIMBORN, S. AND W. K. HÄRDLE (2018): “CRIX an Index for cryptocurrencies,” *Journal of Empirical Finance*, 49, 107–122.

Declaration of Authorship

I hereby confirm that I, Jovanka Matic, have authored this master thesis independently and without use of others than the indicated sources. Where I have consulted the published work of others, in any form (e.g. ideas, equations, figures, text, tables), this is always explicitly attributed.

Berlin, August 30, 2019

Jovanka Matic

Hiermit erkläre ich, Jovanka Matic, dass ich die vorliegende Arbeit allein und nur unter Verwendung der aufgeführten Quellen und Hilfsmittel angefertigt habe. Die Prüfungsordnung ist mir bekannt. Ich habe in meinem Studienfach bisher keine Masterarbeit eingereicht bzw. diese nicht endgültig nicht bestanden.

Berlin, August 30, 2019

Jovanka Matic